HHS Public Access

Author manuscript

J Physiol. Author manuscript; available in PMC 2022 June 01.

Published in final edited form as:

J Physiol. 2021 June ; 599(12): 3101–3119. doi:10.1113/JP281260.

Involvement of TRPC5 Channels, Inwardly Rectifying K^+ channels, PLCβ and PIP_2 in Vasopressin-mediated Excitation of Medial Central Amygdala Neurons

Cody A. Boyle, **Binqi Hu**, **Kati L. Quaintance**, **Saobo Lei***

Department of Biomedical Sciences, School of Medicine and Health Sciences, University of North Dakota, Grand Forks, ND58203, USA

Abstract

Arginine vasopressin (AVP) serves as a hormone in the periphery to modulate water homeostasis and a neuromodulator in the brain to regulate a diverse range of functions including anxiety, social behaviors, cognitive activities and nociception. The amygdala is an essential brain region involved in modulating defensive and appetitive behaviors, pain, and alcohol use disorders. Whereas activation of V_{1a} receptors in the medial nucleus of the central amygdala (CeM) increases neuronal excitability, the involved ionic and signaling mechanisms have not been determined. We found that activation of V_{1a} receptors in the CeM facilitated neuronal excitability predominantly by opening TRPC5 channels, although AVP excited about one-fifth of the CeM neurons via suppressing an inwardly rectifying K^+ (Kir) channel. G proteins and phospholipase Cβ (PLCβ) were required for AVP-elicited excitation of CeM neurons, whereas intracellular Ca^{2+} release and the activity of protein kinase C were unnecessary. Prevention of the depletion of phosphatidylinositol 4,5-bisphosphate (PIP_2) blocked AVP-induced excitation of CeM neurons suggesting that PLCβ-mediated depletion of PIP_2 is involved in AVP-mediated excitation of CeM neurons. Our results may provide a cellular and molecular mechanism to explain the anxiogenic effects of AVP in the amygdala.

Keywords

excitability; action potential; K^+ channels; cation channels; peptide; synapse; depolarization

Introduction

Arginine vasopressin (AVP) or antidiuretic hormone (ADH), is a nonapeptide synthesized primarily by the neurosecretory cells in the paraventricular and supraoptic nuclei of the

*Corresponding author: Saobo Lei (saobo.lei@und.edu).

Authors contributions: All the experiments were performed in the University of North Dakota. S.L. conceived and designed the study. C.A.B. and B.H. were involved in the acquisition, analysis or interpretation of data for the work. K.Q. made data analysis. C.A.B. and S.L. were involved in drafting the work and revising it critically for important intellectual content. All authors approved the final version of the manuscript. All authors agree to be accountable for all aspects of the work in ensuring that questions related to the accuracy or integrity of any part of the work are appropriately investigated and resolved. All persons designated as authors qualify for authorship, and all those who qualify for authorship are listed.

Competing interests:
The Authors declare no conflict of interest.

hypothalamus. In addition to the neurosecretory projections to the posterior pituitary, AVP also travels along the axonal projections from parvocellular neurons of the hypothalamus to discrete extrahypothalamic limbic brain regions including the amygdala and hippocampus (Buijs, 1978; Buijs & Swaab, 1979). AVP functions by interacting with 3 types of receptors: V_{1a}, V_{1b} and V_2 receptors. V_2 receptors are coupled to G_s proteins to upregulate adenylyl cyclase activity resulting in elevation of intracellular cyclic AMP level. V_{1a} and V_{1b} receptors are coupled to $G_{q/11}$ proteins to activate phospholipase Cβ (PLCβ) which hydrolyzes phosphatidylinositol 4,5-bisphosphate (PIP_2), generating inositol trisphosphate (IP_3) to augment intracellular Ca^{2+} release and diacylglycerol (DAG) to activate protein kinase C (PKC). In addition to its hormonal roles in vasoconstriction and antidiuretic action, AVP is also a neuromodulator that regulates a diverse range of functions including anxiety (Caldwell et al., 2008; Neumann & Landgraf, 2012), social behaviors (Cilz et al., 2019; Kompier et al., 2019), learning and memory (de Wied et al., 1993; Caldwell et al., 2008) and nociception (Koshimizu & Tsujimoto, 2009). However, the underlying cellular and molecular mechanisms in the brain have not been fully determined.

The amygdala is an essential brain region involved in modulating defensive (Ressler, 2010; Tye et al., 2011; Dejean et al., 2015; Janak & Tye, 2015) and appetitive (Petrovich, 2011, 2013; Zanchi et al., 2017; Smith & Lawrence, 2018) behaviors, pain (Neugebauer et al., 2004; Veinante et al., 2013; Neugebauer, 2015) and alcohol use disorders (Silberman et al., 2008; Gilpin et al., 2015). The amygdala comprises the lateral amygdala (LA), the basolateral amygdala (BLA), and the central amygdala (CeA). Whilst the LA and BLA contain mostly glutamatergic pyramidal neurons, the CeA is formed majorly by distinct GABAergic neurons and divided into 3 subnuclei named as capsular, lateral, and medial nucleus of CeA (LeDoux, 2000) (abbreviated as CeC, CeL and CeM, respectively). The LA integrates information from the thalamus (LeDoux et al., 1990; Tully et al., 2007), the cortex (McDonald, 1998) and the brainstem (Johansen et al., 2011), and makes glutamatergic synapses onto BLA and CeA neurons. Information flows generally from the LA and BLA into the CeA, although the CeA also receives noxious stimulus information from the brainstem (Bernard et al., 1992; Neugebauer et al., 2009). The LA and BLA send dense glutamatergic projections to the CeA, with the LA projecting only to the CeL and the BLA to both the CeL and the CeM (Krettek & Price, 1978; Pitkanen et al., 1995; Savander et al., 1995). Innervated by GABAergic afferents from other structures as well (Le Gal LaSalle et al., 1978), the CeL and CeM contain local GABA interneurons that may inhibit each other via axon collaterals (Pape & Pare, 2010), and GABAergic projection neurons as amygdala efferents (McDonald & Augustine, 1993; Pare & Smith, 1993). The CeL projects to the CeM, with no reciprocal projection from the CeM to the CeL (Pitkänen, 2000). The CeM is the major output nucleus of the amygdala and projects to regions that produce behavioral and physiologic responses to emotionally relevant events (Hopkins & Holstege, 1978; Pitkänen, 2000; Pape & Pare, 2010), although the CeL also sends GABAergic projections to behavioral and physiologic effector regions (Penzo et al., 2014).

The amygdala receives vasopressinergic innervation from the hypothalamus (Buijs, 1978; Buijs & Swaab, 1979). Vasopressin-producing cells have also been detected in the medial amygdala and the bed nucleus of the stria terminalis, an extended structure of the amygdala (Buijs & Swaab, 1979; Szot & Dorsa, 1993; Rood et al., 2013). The amygdala expresses

vasopressin receptors (Dorsa et al., 1984; Petracca et al., 1986; Veinante & Freund-Mercier, 1997); AVP-binding sites are mainly expressed in the CeM and AVP excites CeM neurons by activation of V_{1a} but not V_{1b} and V_2 receptors (Huber et al., 2005; Bisetti et al., 2006), suggesting that the subtype of the vasopressin receptors in the CeM is V_{1a} receptors. Although microinjection of AVP into the CeA elicits anxiogenic effects (Cragg et al., 2016; Hernandez-Perez et al., 2018), the cellular and molecular mechanisms whereby activation of V_{1a} receptors exerts anxiogenic effects in the CeM have not been determined. In the present study, we found that activation of V_{1a} receptors increases the excitability of CeM neurons primarily via activation of TRPC5 channels, although AVP excites about 20% CeM neurons by depressing the inwardly rectifying K^+ (Kir) channels. PLCβ-mediated depletion of PIP_2 is involved in AVP-elicited excitation in the CeM. Our results may provide a cellular and molecular mechanism whereby AVP exerts anxiogenic effects in the brain.

Materials and Methods

Ethical approval

All procedures and experiments presented in this study were approved by the Institutional Animal Use and Care Committee of the University of North Dakota and performed in accordance with the Guide for the Care and Use of Laboratory Animals published by the National Institutes of Health, USA. All the experiments of the present study also comply with the policy and regulations on animal experimentation of The Journal of Physiology (Grundy, 2015).

Preparation of amygdala slices

Coronal brain slices (300 μm) were prepared from virgin male and female Sprague-Dawley rats (21-35 days old) purchased from Envigo RMS, INC. (Indianapolis, IN), knockout (KO) and wild-type (WT) mice purchased from The Jackson Laboratory. The following 3 strains of KO mice (1-2 months) and their corresponding age-matched WT mice were used: TRPV1 KO mice (B6.129X1-*Trpv1*^{tm1Jul}/J, strain 003770) vs. WT mice (C57BL/6J, strain 000664); TRPC4 KO mice (129S1/SvlmJ-*Trpc4*$^{tm1.1clph}$/J, strain 030802) vs. WT mice (129S1/SvlmJ, strain 002448); TRPC5 KO mice (129S1/SvlmJ-*Trpc5*$^{tm1.1clph}$/J, strain 030804) vs. WT mice (129S1/SvlmJ, strain 002448). The animals were housed in the Center for Biomedical Research in the University of North Dakota with food and water available *ad libitum*. The animal rooms were maintained on a 14/10 h light–dark cycle (lights on at 7:00 a.m.), with a room temperature of 22°C. After being deeply anesthetized with isoflurane, animals were decapitated and their brains were dissected out. The cerebellum was trimmed and the caudal pole of the brain was glued to the plate of a vibrotome (Leica VT1200S). The cutting and recording solution contained (in mM) 130 NaCl, 24 $NaHCO_3$, 3.5 KCl, 1.25 NaH_2PO_4, 2.5 $CaCl_2$, 1.5 $MgCl_2$, and 10 glucose, saturated with 95% O_2 and 5% CO_2 (pH 7.4, adjusted with HCl). Cuttings were made from the rostral pole of the brain and slices were collected from both hemispheres when the structure of amygdala appeared. Slices were kept in the above solution at 35°C until use. All animal procedures conformed to the guidelines approved by the University of North Dakota Animal Care and Use Committee.

Recordings of action potentials, resting membrane potentials and holding currents from CeM neurons

Whole-cell patch-clamp recordings using a Multiclamp 700B amplifier (Molecular Devices, Sunnyvale, CA) in current- or voltage-clamp mode were made from the neurons in the CeM visually identified with infrared video microscopy (Olympus BX51WI) and differential interference contrast optics as described previously (Deng & Lei, 2007; Deng et al., 2010; Li et al., 2019b; Hu et al., 2020). The bath was maintained between 33°C and 34°C by an in-line heater and an automatic temperature controller (TC-324C, Warner Instruments). Slices were perfused with the abovementioned extracellular solution. To exclude the indirect effects of AVP-mediated modulation of synaptic transmission on the excitability of recorded neurons, we included kynurenic acid (1 mM) and picrotoxin (100 μM) in the abovementioned extracellular solution to block glutamatergic and GABAergic transmission, respectively. The recording pipettes contained (in mM) 112 K^+-gluconate, 8 KCl, 2 $MgCl_2$, 40 HEPES, 0.6 EGTA, 2 $ATPNa_2$, 0.4 GTPNa, and 7 phosphocreatine (pH 7.4). Because the CeM neurons did not display spontaneous action potential (AP) firing, a constant positive current was injected to bring the membrane potential close to the threshold to induce sparse AP firing. AVP was dissolved in the extracellular solution at 300 nM, a near-saturating concentration (Huber et al., 2005; Bisetti et al., 2006; Ramanathan et al., 2012), and bath-applied to the slices. To avoid potential desensitization induced by repeated applications of drugs, one slice was limited to only one application of AVP. Data were filtered at 1 kHz, digitized at 10 kHz, acquired on-line and subsequently analyzed using pCLAMP 10.7 software (Molecular Devices, Sunnyvale, CA). APs were detected in Clampfit 10.7 with “Event Detection” and “Threshold Search”. The numbers of APs were binned per min in Excel. For a subset of experiments, we injected a series of positive currents from 30 pA to 330 pA at an increment of 30 pA every 10 s. This protocol was applied to the same cells before and during the application of AVP for 3-5 min because this was the time when the maximal effect of AVP was observed.

For the recordings of resting membrane potentials (RMPs), holding currents (HCs) and voltage-current (V-I) relationship, the extracellular solution was supplemented with tetrodotoxin (TTX, 0.5 μM) to block AP firing. The recording electrodes were filled with the abovementioned K^+-gluconate-containing intracellular solution. HCs were recorded at −60 mV, a membrane potential close to the RMPs of CeM neurons. For V-I relationship, cells were held at −60 mV and stepped from −140 mV to −40 mV or to +20 mV for 400 ms at a voltage increment of 10 mV every 10 s. Steady-state currents were measured within 5 ms prior to the end of the step voltage protocols.

Data analysis and presentation

Data are presented as the means ± SD. Wilcoxon matched-pairs signed rank test (abbreviated as Wilcoxon test in the text), Mann-Whitney test, One-way or Two-way ANOVA was used for statistical analysis as appropriate. The sample number for each experiment was expressed as “n = (number of cells, number of animals)”. Because we recorded data from only one cell in each slice, the cell numbers could also be regarded as the slice numbers. To minimize potential influences of variations from individual animals, each experiment was performed from slices attained from at least 4 animals and One-way

ANOVA was performed to ensure there was no significant difference for the data obtained from individual animals under the same treatment. One-way ANOVA followed by Dunnett's or Tukey's multiple comparison test was used for statistical analysis when the pooled control data were used for comparison. Two-way repeated measures ANOVA followed by Sidak multiple comparison test was used for statistical analysis for the AP firing frequency elicited by injections of positive currents and for the data used to construct the voltage-current relationship. For the comparison of data obtained from KO mice and their corresponding WT mice, both Mann-Whitney test and Ordinary Two-way ANOVA by pooling data from each animal were used for statistical analysis. *P* values were reported throughout the text and significance was set as $P < 0.05$.

Chemicals

[Arg^8]-vasopressin (AVP) was purchased from Bachem. The following chemicals were products of R&D Systems: TTX, kynurenic acid, picrotoxin, SR49059, GDP-β-S, U73122, U73343, heparin, thapsigargin, BAPTA, chelerythrine, bisindolylmaleimide II (Bis II), capsazepine, M084, edelfosine and pyrazolo[1,5-a]pyrimidin-7(4H)-on (QO-58). Dioctanoyl phosphatidylinositol 4,5-bisphosphate (diC8-PIP_2) was purchased from Echelon Biosciences. Drugs were initially prepared in stock solution, aliquoted and stored at −20°C. For those chemicals requiring dimethyl sulfoxide (DMSO) as a solvent, the concentration of DMSO was less than 0.1%. This concentration of DMSO either in the recording pipettes or in the bath had no significant effects on neuronal activity.

Results

AVP augments AP firing frequency in CeM neurons

Whilst previous work has shown that V_{1a} receptor activation facilitates neuronal excitability in the CeM (Huber et al., 2005; Bisetti et al., 2006), the underlying ionic and signaling mechanisms have not been determined. We thus aimed at determining the ionic and signaling mechanisms whereby activation of V_{1a} receptors augments neuronal excitability in the CeM. Because the expression of V_{1a} receptors is restricted to CeM region (Huber et al., 2005), we limited our recordings in this region (Fig. 1A). There are 3 types of neurons in the CeM of rats: low-threshold bursting (LTB, ~71%), regular spiking (RS, ~27%) and late firing (LF, ~2%) (Dumont et al., 2002). The properties of the LTB neurons include spike doublets or bursts in response to depolarizing current pulses and at the break of hyperpolarizing current pulses (Martina et al., 1999; Dumont et al., 2002; Amano et al., 2012). RS neurons generate only single spikes in response to depolarizing current pulses and LF neurons display a conspicuous delay between the onset of suprathreshold depolarizing current pulses and spike discharges. After formation of whole-cell recordings, we injected a series of negative and positive currents to identify the recorded neuronal types (Fig. 1Ba, Ca). Because neurons in the CeM did not show spontaneous AP firing at their RMPs, we injected a persistent positive current to elevate the membrane potentials to just above the firing threshold to induce sparse firing. Out of the 22 CeM neurons recorded, 16 cells were classified as LTB neurons, 6 cells were RS neurons and no LF neurons were met, likely due to their low proportion in the CeM (~2%) (Dumont et al., 2002). Bath application of AVP at 300 nM, a near-saturating concentration (Huber et al., 2005; Bisetti et al., 2006; Ramanathan

et al., 2012), increased the firing frequency in both LTB neurons (Control: 0.17 ± 0.29 Hz, AVP: 1.28 ± 0.84 Hz, n = (16, 6), $P < 0.0001$, Wilcoxon test, Fig. 1Ba–c) and RS neurons (Control: 0.11 ± 0.04 Hz, AVP: 4.23 ± 3.83 Hz, n = (6, 6), $P = 0.031$, Wilcoxon test, Fig. 1Ca–c). There was no significant difference for AVP-induced increase in AP firing ($P = 0.970$, Mann-Whitney test) between LTB neurons (32.9 ± 32.5 fold of control level, n = (16, 6)) and RS neurons (31.5 ± 27.2 fold of control level, n = (6, 6)). AVP exerted equal effects ($P = 0.426$, Mann-Whitney test) on male (Control: 0.19 ± 0.33 Hz, AVP: 1.98 ± 2.19 Hz, n = (11, 3), $P = 0.002$, Wilcoxon test) and female (Control: 0.12 ± 0.13 Hz, AVP: 1.65 ± 1.31 Hz, n = (11, 3), $P = 0.001$, Wilcoxon test) rats. We therefore used both male and female virgin rats for the remaining experiments and the numbers of males and females were kept as equal as possible. We used AVP at 300 nM for each of the remaining experiments because this is a near-saturating concentration (Huber et al., 2005; Bisetti et al., 2006; Ramanathan et al., 2012).

We further tested the effects of AVP on neuronal excitability by injecting a series of positive currents from 30 pA to 330 pA at an increment of 30 pA and a duration of 600 ms (Fig. 2). AVP significantly increased the number of APs recorded from both LTB neurons (n = (13, 6), $F_{(1,12)} = 46.62$, $P < 0.0001$, Two-way repeated measures ANOVA followed by Sidak multiple comparison test, Fig. 2Aa–b) and RS neurons (n = (7, 6), $F_{(1,6)} = 28.01$, $P = 0.002$, Two-way repeated measures ANOVA followed by Sidak multiple comparison test, Fig. 2Ba–b). These results together suggest that AVP augments neuronal excitability of both LTB neurons and RS neurons in the CeM. Because AVP-elicited facilitation of neuronal excitability was not cell-specific, we pooled the data recorded from both LTB and RS neurons for the remaining experiments to identify the underlying ionic and signaling mechanisms.

Activation of V_{1a} receptors depolarizes CeM neurons by opening a cationic channel and inhibiting an inwardly rectifying K^+ channel

We then included TTX (0.5 μM) in the extracellular solution to block AP firing and recorded the RMPs in response to bath application of AVP. Application of AVP depolarized CeM neurons recorded in current clamp (Control: −62.9 ± 3.3 mV, AVP: −58.3 ± 5.4 mV, net depolarization: 4.6 ± 3.5 mV, n = (20, 6), $P < 0.0001$, Wilcoxon test, Fig. 3Aa–b). We also tested the roles of V_{1a} receptors in AVP-mediated depolarization. Slices were pretreated with the selective V_{1a} receptor antagonist, SR49059 (1 μM), and the extracellular solution continuously contained the same concentration of SR49059. Under these circumstances, bath application of AVP failed to alter significantly the AVP-mediated depolarization (SR49059: −64.9 ± 4.4 mV, SR49059 + AVP: −64.7 ± 5.3 mV, net depolarization: 0.24 ± 1.05 mV, n = (8, 4), $P = 0.945$, Wilcoxon test, Fig. 3B), confirming that the effect of AVP was mediated by activation of V_{1a} receptors. In voltage clamp, AVP induced an inward current recorded at −60 mV (−16.6 ± 11.2 pA, n = (16, 5), $P < 0.0001$, Wilcoxon test, Fig. 3Ca–Cb). These results suggest that activation of V_{1a} receptors facilitates neuronal excitability in the CeM by generating membrane depolarization.

We then examined the ionic mechanisms underlying AVP-induced depolarization. Compared with the depolarization induced by AVP in normal extracellular Ca^{2+} concentration,

replacement of extracellular Ca^{2+} with the same concentration of Mg^{2+} significantly increased AVP-elicited depolarization (Control: −60.7 ± 3.5 mV, AVP: −50.3 ± 11.7 mV, net depolarization: 10.4 ± 11.4 mV, n = (27, 7), P <0.0001, Wilcoxon test; P = 0.0445 vs. the effect of AVP in normal extracellular Ca^{2+} concentration, One-way ANOVA followed by Dunnett's test, Fig. 3Da, Dc), suggesting that removal of extracellular Ca^{2+} augments AVP-mediated depolarization. We further tested the roles of intracellular Ca^{2+} by including BAPTA (10 mM) in the recording pipettes to chelate intracellular Ca^{2+}. Inclusion of BAPTA in the recording pipettes failed to alter AVP-induced depolarization significantly (Control: −63.1 ± 4.4 mV, AVP: −58.2 ± 5.4 mV, net depolarization: 4.8 ± 2.6 mV, n = (7, 4), P = 0.016, Wilcoxon test; P = 0.998 vs. the control effect of AVP, One-way ANOVA followed by Dunnett's test, Fig. 3Db–c). These results suggest that AVP-mediated depolarization is not dependent on intracellular Ca^{2+}.

We further determined the ionic mechanisms whereby V_{1a} receptor activation depolarizes CeM neurons by measuring the voltage-current (V-I) relationship of the currents generated by AVP. Cells were held at −60 mV and stepped from −140 mV to −40 mV for 400 ms at a voltage step of 10 mV every 10 s. Steady-state currents were measured within 5 ms prior to the end of the step voltage protocol. Under these circumstances, AVP elicited a persistent inward current at the voltages between −140 mV and −40 mV in 24 cells out of the 30 cells recorded (from 8 rats) (Fig. 4Aa–c). The remaining 6 cells displayed a V-I curve of inwardly rectifying K^+ (Kir) channels with a reversal potential at −96.4 ± 11.6 mV (n = 6 cells) (Fig. 4Ba–c). These results suggest that activation of V_{1a} receptors excites CeM neurons by opening a cationic channel in ~80% (24/30) neuronal population and inhibiting Kir channels in ~20% (6/30) neuronal population.

We further extended the voltage range to +20 mV to measure the reversal potential of the cationic currents elicited by AVP in the continuous presence of $BaCl_2$ (300 μM) to block potential contamination of the Kir channels. In addition to 300 μM $BaCl_2$, the extracellular solution also contained TTX (0.5 μM) to block voltage-gated Na^+ channels, $CdCl_2$ (200 μM) and $NiCl_2$ (1 mM) to block voltage-gated Ca^{2+} channels. Under these circumstances, AVP-elicited net currents showed a reversal potential of −34.4 ± 9.6 mV with double rectifications (n = (7, 4), Fig. 4Ca–c), further confirming the involvement of cationic channels.

TRPC5 channels are involved in V_{1a} receptor-mediated depolarization

The V-I curve of AVP-elicited currents (Fig. 4Cc) resembles that of TRPV1, TRPC4 and TRPC5 channels (Wu et al., 2010). The amygdala expresses TRPV1 (Zschenderlein et al., 2011; Xiao et al., 2016), TRPC4 (Riccio et al., 2014) and TRPC5 (Riccio et al., 2009) channels. We next tested the roles of these channels in AVP-mediated depolarization of CeM neurons using their selective pharmacological blockers and KO mice. Application of the TRPV1 blocker, capsazepine (10 μM), did not significantly alter AVP-elicited depolarization (Capsazepine: −62.9 ± 4.4 mV, Capsazepine + AVP: −58.5 ± 5.3 mV, net depolarization: 4.3 ± 3.3 mV, n = (18, 6), P < 0.0001, Wilcoxon test; P = 0.883 vs. AVP alone, Mann-Whitney test, Fig. 5A, D). Likewise, application of AVP induced significant depolarization of CeM neurons in slices cut from WT mice (Control: −62.8 ± 2.7 mV, AVP: −58.8 ± 2.5 mV, net depolarization: 4.0 ± 1.5 mV, n = (14, 4), P = 0.0001, Wilcoxon test, Fig. 5B, D) or TRPV1

KO mice (Control: −64.6 ± 6.4 mV, AVP: −61.2 ± 6.9 mV, net depolarization: 3.4 ± 1.6 mV, n = (21, 6), P<0.0001, Wilcoxon test, Fig. 5C–D). There was no significant difference (P = 0.249, Mann-Whitney test; $F_{(1,30)}$ = 1.31, P = 0.261, Ordinary Two-way ANOVA) for the AVP-elicited net depolarization of CeM neurons between WT mice (4.0 ± 1.5 mV, n = (14, 4)) and TRPV1 KO mice (3.4 ± 1.6 mV, n = (21, 6), Fig. 5D). These data collectively suggest that TRPV1 channels are not involved in AVP-induced excitation of CeM neurons.

We then probed the roles of TRPC4/5 channels in AVP-elicited depolarization of CeM neurons. Bath application of the selective TRPC4/5 channel blocker, M084 (100 μM) (Yang et al., 2015; Zhu et al., 2015), did not significantly alter RMPs (Control: −64.9 ± 4.3 mV, M084: −64.3 ± 5.5 mV, net change: 0.7 ± 4.4 mV, n = (15, 4), P = 0.639, Wilcoxon test), but significantly attenuated AVP-mediated depolarization (M084: −64.3 ± 5.5 mV, M084 + AVP: −63.0 ± 5.8 mV, net depolarization: 1.2 ± 1.1 mV, n = (15, 4), P = 0.001, Wilcoxon test; P = 0.007 vs. AVP alone, Mann-Whitney test, Fig. 5E, J), suggesting that TRPC4/5 channels are involved in AVP-elicited depolarization of CeM neurons. We then used TRPC4 and TRPC5 KO mice to further determine the roles of TRPC4 and TRPC5 channels. Application of AVP evoked comparable depolarizations in slices cut from WT mice (Control: −61.1 ± 5.2 mV, AVP: −56.2 ± 6.9 mV, n = (14, 4), P = 0.0001, Wilcoxon test, Fig. 5F, J) and TRPC4 KO mice (Control: −64.1 ± 4.6 mV, AVP: −60.3 ± 5.5 mV, n = (14, 5), P = 0.0001, Wilcoxon test, Fig. 5G, J). AVP-elicited net depolarization was not significantly different (P = 0.322, Mann-Whitney test; $F_{(1,23)}$ = 0.49, P = 0.489, Ordinary Two-way ANOVA) between WT mice (4.9 ± 3.3 mV, n = (14, 4)) and TRPC4 KO mice (3.8 ± 3.5 mV, n = (14, 5)), suggesting that TRPC4 channels are not essential for AVP-mediated depolarization. However, AVP induced a significantly smaller depolarization of CeM neurons in slices cut from TRPC5 KO mice (Control: −62.2 ± 2.7 mV, AVP: −60.8 ± 2.8 mV, net depolarization: 1.4 ± 1.1 mV, n = (17, 5), P < 0.0001, Wilcoxon test), compared with WT mice (Control: −63.1 ± 3.8 mV, AVP: −58.1 ± 2.6 mV, net depolarization: 5.0 ± 2.6 mV, n = (12, 4), P = 0.0005, Wilcoxon test; WT mice vs. TRPC5 KO mice: P < 0.0001 Mann-Whitney test, $F_{(1,24)}$ = 22.12, P < 0.0001, Ordinary Two-way ANOVA, Fig. 5H–J). One would argue that decrease in AVP-elicited depolarization in TRPC5 KO mice may be due to a reduced expression of V_{1a} receptors in TRPC5 KO mice, irrelevant to TRPC5 channels. To exclude this possibility, we performed a positive control experiment. Because we showed previously that activation of V_{1a} receptors excites CA1 interneurons by inhibiting a K^+ channel (Ramanathan et al., 2012), we recorded and compared the AVP-induced changes of holding currents from CA1 interneurons in slices cut from TRPC5 KO mice and WT mice. Application of AVP elicited comparable (P = 0.470, Mann-Whitney test; $F_{(1,23)}$ = 0.88, P = 0.359, Ordinary Two-way ANOVA) inward currents recorded from CA1 interneurons in slices cut from TRPC5 KO mice (-20.0 ± 9.0 pA, n = (16, 4)) and WT mice (-17.3 ± 9.1 pA, n = (15, 4), data not shown), arguing against the notion that the decreased level of AVP-elicited depolarization of CeM neurons is due to the reduction of V_{1a} receptor expression in TRPC5 KO mice.

PLCβ is involved in AVP-elicited excitation of CeM neurons

Because V_{1a} receptors are coupled to $G_{q/11}$, we tested the roles of G proteins in AVP-mediated depolarization. Intracellular dialysis of the G protein inactivator, GDP-β-S (0.5

mM) blocked AVP-elicited depolarization (Control: −61.0 ± 3.1 mV, AVP: −60.4 ± 2.8 mV, net depolarization: 0.61 ± 0.89 mV, n = (9, 4), $P = 0.098$, Wilcoxon test; $P = 0.002$ vs. AVP alone, One-way ANOVA followed by Tukey's test, Fig. 6A, E), indicating the requirement of G proteins. Activation of V_{1a} receptors increases the function of PLCβ resulting in hydrolysis of PIP_2 to generate IP_3 to increase intracellular Ca^{2+} release and DAG to activate PKC. We next tested the roles of these intracellular signals in AVP-elicited depolarization of CeM neurons. Slices were pretreated with the selective PLC inhibitor, U73122 (5 μM), for >2 h. Application of AVP to the slices pretreated with U73122 did not significantly depolarize CeM neurons (Control: −63.3 ± 4.5 mV, AVP: −63.1 ± 5.1 mV, n = (14, 5), $P = 0.502$, Wilcoxon test, Fig. 6B, E), whereas AVP still significantly depolarized CeM neurons in slices pretreated with the inactive analog, U73343 (5 μM) (Control: −60.1 ± 2.5 mV, AVP: −55.3 ± 2.5 mV, n = (10, 4), $P = 0.002$, Wilcoxon test, Fig. 6C, E). There was significant difference ($P = 0.001$, One-way ANOVA followed by Tukey's test) for AVP-induced net depolarization obtained from cells pretreated with U73122 (0.22 ± 1.53 mV, n = 14 cells) and U73343 (4.8 ± 1.8 mV, n = 10 cells, Fig. 6E). Similarly, pretreatment of slices with edelfosine (15 μM), another PLC inhibitor, significantly attenuated AVP-elicited depolarization (Control: −62.8 ± 3.4 mV, AVP: −61.7 ± 3.7 mV, net depolarization: 1.2 ± 3.7 mV, n = (11, 4), $P = 0.032$, Wilcoxon test; $P = 0.001$ vs. AVP alone, One-way ANOVA followed by Tukey's test, Fig. 6D–E). These results together suggest that PLCβ is required for V_{1a} receptor-mediated excitation of CeM neurons.

IP_3 receptors and PKC are not involved in AVP-mediated depolarization

We probed the roles of intracellular Ca^{2+} release in AVP-induced depolarization of CeM neurons. Intracellular dialysis of heparin (2 mg/ml), a blocker for IP_3 receptors, via the recording pipettes, did not significantly alter AVP-mediated depolarization (Control: −61.6 ± 3.3 mV, AVP: −52.0 ± 13.1 mV, net depolarization: 6.1 ± 4.5 mV, n = (10, 4), $P = 0.002$, Wilcoxon test; $P = 0.890$ vs. AVP alone, One-way ANOVA followed by Dunnett's test, Fig. 7A, F), suggesting that Ca^{2+} release from the IP_3-sensitive store is not required for AVP-elicited depolarization. Moreover, intracellular perfusion of thapsigargin (10 μM), a non-competitive inhibitor of the sarco/endoplasmic reticulum Ca^{2+} ATPase, via the recording pipettes, did not significantly modify AVP-mediated depolarization (Control: −63.8 ± 4.6 mV, AVP: −58.7 ± 5.4 mV, net depolarization: 5.1 ± 2.7 mV, n = (10, 4), $P = 0.002$, Wilcoxon test; $P = 0.999$ vs. AVP alone, One-way ANOVA followed by Dunnett's test, Fig. 7B, F). These results suggest that intracellular Ca^{2+} release is not required for AVP-elicited depolarization.

We then examined the roles of PKC in AVP-induced excitation of CeM neurons. Slices were pretreated with bisindolylmaleimide II (Bis II, 1 μM), a specific PKC inhibitor, and the extracellular solution continuously contained the same concentration of Bis II. Under these circumstances, bath application of AVP to the slices treated with Bis II still induced a comparable depolarization of CeM neurons (Control: −64.5 ± 4.9 mV, AVP: −58.8 ± 7.3 mV, net depolarization: 5.6 ± 5.2 mV, n = (16, 5), $P < 0.0001$, Wilcoxon test; $P = 0.967$ vs. AVP alone, One-way ANOVA followed by Dunnett's test, Fig. 7C, F). Likewise, pretreatment of slices with and continuous bath application of chelerythrine (10 μM), another specific PKC inhibitor, failed to significantly modify AVP-mediated depolarization (Control: −63.3 ± 7.8

mV, AVP: −57.4 ± 10.7 mV, net depolarization: 5.9 ± 4.7, n = (12, 4), $P = 0.0005$, Wilcoxon test; $P = 0.936$ vs. AVP alone, One-way ANOVA followed by Dunnett's test, Fig. 7D, F). These results together suggest that PKC is not involved in AVP-elicited depolarization.

Roles of PIP_2 in AVP-elicited depolarization of CeM neurons

We then tested the hypothesis that activation of V_{1a} receptors increases the function of PLCβ resulting in depletion of PIP_2 to depolarize CeM neurons because PIP_2 has been shown to regulate the functions of a variety of ion channels (Suh & Hille, 2008; Rodriguez-Menchaca et al., 2012). We included the water-soluble diC8-PIP_2 (20 μM) in the recording pipettes to compensate for the depletion of PIP_2 in response to PLCβ activation. Supplementation of diC8-PIP_2 blocked AVP-mediated depolarization (Control: −60.5 ± 2.8 mV, AVP: −59.9 ± 3.5 mV, net depolarization: 0.6 ± 1.3 mV, n = (12, 4), $P = 0.176$, Wilcoxon test; $P = 0.008$ vs. AVP alone, One-way ANOVA followed by Dunnett's test, Fig. 7E–F), suggesting that depletion of PIP_2 is involved in V_{1a} receptor-mediated depolarization of CeM neurons.

Roles of PIP_2 depletion, TRPC5 and Kir channels in V_{1a} receptor-elicited increases in AP firing

We further tested whether PIP_2 depletion is involved in V_{1a} receptor-mediated augmentation of AP firing frequency. Dialysis of diC8-PIP_2 (20 μM) into the CeM neurons prevented AVP-induced increases in AP firing elicited by injection of a series of positive currents (n = (13, 4), $F_{(1,12)} = 4.38$, $P = 0.058$, Two-way repeated measures ANOVA followed by Sidak multiple comparison test, Fig. 8Aa–b), suggesting that PLCβ-mediated depletion of PIP_2 is required for AVP-elicited excitation of CeM neurons. We noticed that the AP numbers of the CeM neurons dialyzed intracellularly with diC8-PIP_2 were significantly higher than those of the CeM neurons in control condition without dialysis of diC8-PIP_2 ($F_{(1,341)} = 20.84$, $P < 0.0001$, Ordinary Two-way ANOVA followed by Sidak multiple comparison test, Fig. 8Ac). Increases in basal AP numbers in the presence of diC8-PIP_2 alone may have exerted temporal limitation for AVP to augment AP firing numbers further. To exclude this possibility, we used QO-58, an activator of Kv7 (KCNQ) channels (Zhang et al., 2013). Kv7 channels are expressed in rat central amygdala neurons and application of QO-58 augmented M-currents (Sheng et al., 2021). In the CeM neurons dialyzed with diC8-PIP_2, application of QO-58 (15 μM) significantly depressed the number of APs (n = (12, 4), $F_{(1,11)} = 137.7$, $P < 0.0001$, Two-way repeated measures ANOVA followed by Sidak multiple comparison test, Fig. 8Ad). In the continuous presences of both QO-58 and diC8-PIP_2, following application of AVP failed to enhance AP firing numbers significantly (n = (12, 4), $F_{(1,11)} = 2.23$, $P = 0.164$, Two-way repeated measures ANOVA followed by Sidak multiple comparison test, Fig. 8Ad). Because TRPC5 channels are required for AVP-induced depolarization, we also tested whether TRPC5 channels are required for AVP-elicited augmentation of AP firing by using the TRPC5 KO mice. Application of AVP significantly increased the number of APs elicited by injections of the positive currents in slices cut from WT mice (n = (15, 5), $F_{(1,14)} = 45.5$, $P < 0.0001$, Two-way repeated measures ANOVA followed by Sidak multiple comparison test, Fig. 8Ba–b), whereas AVP failed to enhance AP numbers significantly in slices cut from TRPC5 KO mice (n = (15, 5), $F_{(1,14)} = 2.46$, $P = 0.139$, Two-way repeated measures ANOVA followed by Sidak multiple comparison test, Fig. 8Bc–d), further confirming that TRPC5 channels are required for V_{1a} receptor-mediated enhancement of AP

firing. Because the basal AP firing numbers in slices cut from TRPC5 KO mice were significantly higher than those of WT mice ($F_{(1,308)}$ = 137.6, P < 0.0001, Ordinary Two-way ANOVA followed by Sidak multiple comparison test, Fig. 8Be), the ineffectiveness of AVP in slices cut from TRPC5 KO mice could be due to the higher basal AP firing numbers of CeM neurons in TRPC5 KO mice. Similarly, we included QO-58 in the extracellular solution to lower the basal level of AP firing numbers in response to the positive current injection protocol. Bath application of QO-58 (20 μM) significantly decreased AP firing numbers in slices cut from TRPC5 KO mice (n = (12, 4), $F_{(1,11)}$ = 153, P < 0.0001, Two-way repeated measures ANOVA followed by Sidak multiple comparison test, Fig. 8Bf). However, in the presence of QO-58, application of AVP still failed to enhance AP firing numbers significantly in TRPC5 KO mice (n = (12, 4), $F_{(1,11)}$ = 0.78, P = 0.397, Two-way repeated measures ANOVA followed by Sidak multiple comparison test, Fig. 8Bf). Because AVP excited ~20% rat CeM neurons primarily by depressing Kir channels, we included M084 (100 μM) in the extracellular solution to block TRPC5 channels and to isolate the contribution of Kir channels in AVP-induced augmentation of AP firing frequency in rats. In the presence of M084, application of AVP enhanced AP firing numbers only when the injection currents were from 90 to 150 pA (n = (15, 4), Fig. 8Ca–b), suggesting that Kir channels partially contributed to AVP-elicited excitation of rat CeM neurons. Based on our experimental results, we proposed a schematic diagram to summarize the ionic and signaling mechanisms whereby activation of V_{1a} receptors excites CeM neurons (Fig. 9).

Discussion

Whilst it has been shown that microinjection of AVP into the CeA elicits anxiogenic effects (Cragg et al., 2016; Hernandez-Perez et al., 2018) and activation of V_{1a} receptors in the CeM increases neuronal excitability (Huber et al., 2005; Bisetti et al., 2006), the underlying ionic and signaling mechanisms have not been determined. As shown in Figure 9, we found that activation of V_{1a} receptors excites the majority (80%) of CeM neurons primarily by opening TRPC5 channels, although AVP excites about 20% of CeM neurons majorly by depressing a Kir channel. The V_{1a} receptor-mediated excitation of CeM neurons depends on PLCβ-mediated depletion of PIP_2 without the requirements of intracellular Ca^{2+} release and PKC.

Activation of cationic channels and inhibition of resting K^+ channels are two major ionic mechanisms whereby neuromodulators facilitate neuronal excitability. Our results suggest that V_{1a} receptor activation excites CeM neurons predominantly by opening a cationic conductance because the V-I curve of the AVP-induced currents reversed at about −34 mV and resembled that of TRPV1, TRPC4 or TRPC5 channels (Wu et al., 2010). Whereas capsazepine is a TRPV1 blocker, application of capsazepine failed to block AVP-mediated depolarization. Consistent with the pharmacological experiments, AVP-elicited depolarization recorded from TRPV1 KO mice was comparable to that attained from WT mice, excluding the involvement of TRPV1 channels. In congruence with the electrophysiological results, TRPV1 channels are distributed majorly in LA and BLA (Zschenderlein et al., 2011; Xiao et al., 2016) with less expression in CeA (Zschenderlein et al., 2011). M084 is a blocker for TRPC4/5 channels (Yang et al., 2015; Zhu et al., 2015). Our result that application of M084 significantly reduced AVP-elicited depolarization

indicates the involvement of TRPC4/5 channels. AVP induced a significantly smaller depolarization in slices cut from TRPC5 KO mice, whereas AVP elicited a comparable depolarization of CeM neurons in slices cut from TRPC4 KO mice, suggesting the requirement of TRPC5 channels. Both TRPC4 and TRPC5 channels are distributed in the amygdala with TRPC4 channels expressed in the LA and BLA (Riccio et al., 2014) and TRPC5 channels in the LA, BLA and CeA (Riccio et al., 2009). The localization of TRPC5 channels in the CeA further supports a role of TRPC5 channels in AVP-induced depolarization. However, our results that removal of extracellular Ca^{2+} significantly increased AVP-elicited depolarization of CeM neurons seem incongruous with the results showing that elevation of extracellular Ca^{2+} augments TRPC5 currents in transfected cells (Okada et al., 1998; Chen et al., 2017). In HEK cells transfected with TRPC5 cDNA initially cloned from mouse brain (Okada et al., 1998), elevation of extracellular Ca^{2+} from 1.2 mM dubbed as "0Ca^{2+}" in the work to 10 mM increased TRPC5 channel currents. Because 1.2 mM Ca^{2+} is close to the physiological extracellular Ca^{2+} concentration and 10 mM extracellular Ca^{2+} is almost not physiological, these results may at most suggest that pharmacological elevation of extracellular Ca^{2+} enhances TRPC5 channel currents. In the recent work (Chen et al., 2017), elevation of extracellular Ca^{2+} from 0 Ca^{2+} to 2 mM increased TRPC5 channel currents. However, consistent with our results, extracellular Ca^{2+} is well known to reduce the monovalent cation currents of many Ca^{2+}-permeable cation channels (Helliwell & Large, 1996; Owsianik et al., 2006; Arichi et al., 2019). In the isolated rat intracardiac ganglion neurons, activation of another peptide receptor, the bradykinin B_2 receptor, resulted in depolarization by opening a nonselective cation channel sensitive to the TRPC4/5 channel blocker, ML204 (Arichi et al., 2019). Removal of extracellular Ca^{2+} markedly increased the bradykinin-induced currents, suggesting that extracellular Ca^{2+} exerted inhibitory effects on the putative TRPC4/5 channels (Arichi et al., 2019). If elevation of extracellular Ca^{2+} indeed augments TRPC5 channel currents in physiological condition, there are several reasons to explain the discrepant results between neurons and transfected cells. First, many neurons express Ca^{2+}-sensed nonselective cation channels and lowering extracellular Ca^{2+} can open this type of cation channels (Xiong et al., 1997). If activation of V_{1a} receptors also exerts effects on Ca^{2+}-sensed nonselective cation channels, removing extracellular Ca^{2+} could potentially augment AVP-elicited depolarization by interacting with the Ca^{2+}-sensed nonselective cation channels. Second, removing extracellular Ca^{2+} could potentially increase the potency of V_{1a} receptors in the CeM neurons, although depletion of extracellular Ca^{2+} has no effects on V_{1a} receptor-induced increases in inward currents in CA1 interneurons of the hippocampus (Ramanathan et al., 2012), arguing against a potentiating effect of extracellular Ca^{2+} depletion on V_{1a} receptor function. Third, the components of the intracellular solutions used are different. For the experiments performed on transfected cells, the intracellular solution contained Cs^+, high concentration of EGTA (10 mM) and low concentration of HEPES (10 mM) (Chen et al., 2017), whereas our experiments were performed by using K^+-containing internal solution supplemented with low concentration of EGTA (0.6 mM) and higher concentration of HEPES (40 mM). EGTA is a well-known Ca^{2+} chelator likely affecting intracellular Ca^{2+} level. Fourth, because our results also indicated that depression of K^+ channels is another ionic mechanism involved in the depolarization of CeM neurons in response to V_{1a} receptor activation, the altered contribution of K^+ channels in AVP-induced increases in

depolarization in zero extracellular Ca^{2+} solution cannot be excluded. Nevertheless, our results support the involvement of TRPC5 channels in AVP-elicited excitation of CeM neurons.

Our results suggest that Kir channels are involved in V_{1a} receptor-mediated excitation of a small population (20%) of rat CeM neurons. Kir channels are divided into four functional groups including Kir2, Kir3 (G protein-gated inwardly rectifying potassium (GIRK) channels), Kir6 (ATP-sensitive K^+ (K_{ATP}) channels) and K^+ transport channels (Hibino et al., 2010). Whilst V_{1a} receptor activation has been shown to inhibit K_{ATP} channels (Wakatsuki et al., 1992; Shi et al., 2007), it is unlikely that the K_{ATP} channels are the target for V_{1a} receptors in the CeM neurons because our recording pipettes contained 2 mM ATP which should have effectively blocked the K_{ATP} channels. Because AVP excites CeM neurons via inhibition of Kir channels in only about one-fifth of the cell population, it is difficult to isolate and identify the involved subtype of the Kir channels in the CeM. Nonetheless, our results showed that Kir channels may contribute partially to AVP-elicited excitation of CeM neurons in rats because AVP still induced significant increase in AP firing number when low intensities of positive currents were injected in the extracellular solution containing M084 to block TRPC5 channels.

V_{1a} receptors are coupled to $G_{q/11}$ proteins resulting in increases in the function of PLCβ which hydrolyses PIP_2 to generate IP_3 to elevate intracellular Ca^{2+} release and DAG to activate PKC. Our results suggest that the functions of PLCβ and PIP_2 are required for V_{1a} receptor-elicited excitation of CeM neurons. Because we showed that TRPC5 and Kir channels are involved in V_{1a} receptor-induced excitation, it is reasonable to speculate that PLCβ and PIP_2 interact with TRPC5 and Kir channels to excite CeM neurons. Activation of $G_{q/11}$-coupled receptors results in activation of TRPC5 channels (Plant & Schaefer, 2005; Rohacs, 2013). TRPC5 activation elicited by $G_{q/11}$-coupled receptors depends upon PLCβ, but evidently did not involve IP_3 or DAG (Schaefer et al., 2000). Inhibition of IP_3 receptors with intracellular infusion of heparin failed to affect receptor-mediated activation of currents in cells transfected with TRPC4 and TRPC5 channels (Plant & Schaefer, 2005). TRPC5 could still be activated via a muscarinic receptor in DT-40 B cells lacking all three IP_3 receptor subtypes (Venkatachalam et al., 2003). Like homomeric TRPC4 and TRPC5 channels, heteromers formed between TRPC1 and TRPC5, were not activated by infusion of IP_3 but responded to subsequent muscarinic receptor activation (Strubing et al., 2001). Furthermore, DAG was not involved in the activation of TRPC5 channels in response to $G_{q/11}$-coupled receptors (Hofmann et al., 1999; Venkatachalam et al., 2003). Consistent with this scenario, our results suggest that V_{1a} receptor-mediated excitation of CeM neurons is independent of IP_3 receptors, intracellular Ca^{2+} release, DAG and PKC.

PIP_2 has been shown to modulate the functions of diverse ion channels (Suh & Hille, 2008; Rodriguez-Menchaca et al., 2012). TRPC4 and TRPC5 channels are also subject to PIP_2 modulation. TRPC4α but not TRPC4β was strongly inhibited by intracellularly applied PIP_2 (Otsuguro et al., 2008). Depletion of PIP_2 activates TRPC5 channels, whereas intracellular perfusion of PIP_2 via the patch pipettes inhibited TRPC5 currents expressed in HEK293 cells (Trebak et al., 2009). In the present study, we further showed that depletion of PIP_2 is involved in AVP-mediated depolarization of CeM neurons. Because TRPC5 channels are the

predominant channels mediating AVP-induced excitation of CeM neurons, it is reasonable to speculate that activation of V_{1a} receptors activates TRPC5 channels by PLCβ-mediated depletion of PIP_2, resulting in excitation of CeM neurons.

Our results showed that activation of V_{1a} receptors excited one-fifth of CeM neurons principally via inhibition of Kir channels. Because PIP_2 is involved in V_{1a} receptor-mediated excitation of CeM neurons, it is rational to reason that PIP_2 is also involved in V_{1a} receptor-elicited depression of Kir channels. Consistent with this scenario, Kir channels are activated by PIP_2 (Huang et al., 1998; Suh & Hille, 2008; Li et al., 2019a), but inhibited by PLCβ-mediated depletion of PIP_2 (Cho et al., 2001; Meyer et al., 2001; Cho et al., 2005).

Amygdala is a principal structure involved in fear and anxiety. LA receives multimodal sensory information from the thalamus and cortex, serving as the major sensory interface. The CeM is the principal output station, as its projection neurons contact different structures in the brainstem and in the hypothalamus to orchestrate conditioned autonomic and motor responses (Ehrlich et al., 2009). Facilitation of neuronal excitability in the CeM generally augments anxiety and fear responses. The neuropeptide vasopressin is a modulator of mammalian social behavior and emotion, particularly fear, aggression, and anxiety (Bielsky et al., 2004). Strong evidence demonstrates that anxiety disorders and fear responses are associated with elevated AVP functions (Bielsky et al., 2004; Egashira et al., 2007; Egashira et al., 2009; Mak et al., 2012). It is generally believed that V_{1a} receptors are responsible for AVP-mediated anxiogenic effects and fear responses. For instance, V_{1a} receptor KO mice showed reduced anxiety-like behaviors (Bielsky et al., 2004; Egashira et al., 2007), whereas overexpression of V_{1a} receptors facilitated anxiety-like responses (Bielsky et al., 2005). Infusion of V_{1a} receptor antisense into the brain (Landgraf et al., 1995) or central administration of V_{1a} receptor antagonists (Liebsch et al., 1996; Mak et al., 2012) induced anxiolytic effects. Polymorphisms of both AVP (Murgatroyd et al., 2004) and V_{1a} receptors (Hammock et al., 2005) are correlated with anxiety-like behaviors. Although microinjection of AVP into the CeA elicits anxiogenic effects (Cragg et al., 2016; Hernandez-Perez et al., 2018), the cellular and molecular mechanisms whereby AVP exerts the anxiogenic effects have not been determined. Our results suggest that activation of V_{1a} receptors excites CeM neurons by activation of TRPC5 channels and depression of Kir channels. Consistent with our results, activation of TRPC5 channels elevates fear and anxiety response (Riccio et al., 2009; Just et al., 2018). Kir channels such as the GIRK channels are also involved in anxiety response (Blednov et al., 2001; Pravetoni & Wickman, 2008; Wydeven et al., 2014). Our results also showed that PLCβ-mediated depletion of PIP_2 is involved in V_{1a} receptor-mediated excitation of CeM neurons. In conformity with our results, PLCβ is involved in anxiety responses (McOmish et al., 2008; Xiao et al., 2012). Our results therefore provide a cellular and molecular mechanism by which potential therapeutic strategies could be developed.

Supplementary Material

Refer to Web version on PubMed Central for supplementary material.

Funding:

This work was supported by the National Institute Of General Medical Sciences (NIGMS) and National Institute Of Mental Health (NIMH) grant R01MH118258 to S.L.

Data Availability Statement:

The data that support the findings of this study are available from the corresponding author upon reasonable request.

References

Amano T, Amir A, Goswami S & Pare D. (2012). Morphology, PKCdelta expression, and synaptic responsiveness of different types of rat central lateral amygdala neurons. J Neurophysiol 108, 3196–3205. [PubMed: 22972957]

Arichi S, Sasaki-Hamada S, Kadoya Y, Ogata M & Ishibashi H. (2019). Excitatory effect of bradykinin on intrinsic neurons of the rat heart. Neuropeptides 75, 65–74. [PubMed: 31047706]

Bernard JF, Huang GF & Besson JM. (1992). Nucleus centralis of the amygdala and the globus pallidus ventralis: electrophysiological evidence for an involvement in pain processes. J Neurophysiol 68, 551–569. [PubMed: 1527575]

Bielsky IF, Hu SB, Ren X, Terwilliger EF & Young LJ. (2005). The V1a vasopressin receptor is necessary and sufficient for normal social recognition: a gene replacement study. Neuron 47, 503–513. [PubMed: 16102534]

Bielsky IF, Hu SB, Szegda KL, Westphal H & Young LJ. (2004). Profound impairment in social recognition and reduction in anxiety-like behavior in vasopressin V1a receptor knockout mice. Neuropsychopharmacology 29, 483–493. [PubMed: 14647484]

Bisetti A, Cvetkovic V, Serafin M, Bayer L, Machard D, Jones BE & Muhlethaler M. (2006). Excitatory action of hypocretin/orexin on neurons of the central medial amygdala. Neuroscience 142, 999–1004. [PubMed: 16996221]

Blednov YA, Stoffel M, Chang SR & Harris RA. (2001). GIRK2 deficient mice. Evidence for hyperactivity and reduced anxiety. Physiol Behav 74, 109–117. [PubMed: 11564458]

Buijs RM. (1978). Intra- and extrahypothalamic vasopressin and oxytocin pathways in the rat. Pathways to the limbic system, medulla oblongata and spinal cord. Cell Tissue Res 192, 423–435. [PubMed: 699026]

Buijs RM & Swaab DF. (1979). Immuno-electron microscopical demonstration of vasopressin and oxytocin synapses in the limbic system of the rat. Cell Tissue Res 204, 355–365. [PubMed: 527026]

Caldwell HK, Lee HJ, Macbeth AH & Young WS 3rd. (2008). Vasopressin: behavioral roles of an “original” neuropeptide. Prog Neurobiol 84, 1–24. [PubMed: 18053631]

Chen X, Li W, Riley AM, Soliman M, Chakraborty S, Stamatkin CW & Obukhov AG. (2017). Molecular Determinants of the Sensitivity to Gq/11-Phospholipase C-dependent Gating, Gd3+ Potentiation, and Ca2+ Permeability in the Transient Receptor Potential Canonical Type 5 (TRPC5) Channel. J Biol Chem 292, 898–911. [PubMed: 27920205]

Cho H, Lee D, Lee SH & Ho WK. (2005). Receptor-induced depletion of phosphatidylinositol 4,5-bisphosphate inhibits inwardly rectifying K+ channels in a receptor-specific manner. Proc Natl Acad Sci U S A 102, 4643–4648. [PubMed: 15767570]

Cho H, Nam GB, Lee SH, Earm YE & Ho WK. (2001). Phosphatidylinositol 4,5-bisphosphate is acting as a signal molecule in alpha(1)-adrenergic pathway via the modulation of acetylcholine-activated K(+) channels in mouse atrial myocytes. J Biol Chem 276, 159–164. [PubMed: 11029461]

Cilz NI, Cymerblit-Sabba A & Young WS. (2019). Oxytocin and vasopressin in the rodent hippocampus. Genes Brain Behav 18, e12535. [PubMed: 30378258]

Cragg B, Ji G & Neugebauer V. (2016). Differential contributions of vasopressin V1A and oxytocin receptors in the amygdala to pain-related behaviors in rats. Mol Pain 12.

de Wied D, Diamant M & Fodor M. (1993). Central nervous system effects of the neurohypophyseal hormones and related peptides. Front Neuroendocrinol 14, 251–302. [PubMed: 8258377]

Dejean C, Courtin J, Rozeske RR, Bonnet MC, Dousset V, Michelet T & Herry C. (2015). Neuronal Circuits for Fear Expression and Recovery: Recent Advances and Potential Therapeutic Strategies. Biol Psychiatry 78, 298–306. [PubMed: 25908496]

Deng PY & Lei S. (2007). Long-term depression in identified stellate neurons of juvenile rat entorhinal cortex. J Neurophysiol 97, 727–737. [PubMed: 17135466]

Deng PY, Xiao Z, Jha A, Ramonet D, Matsui T, Leitges M, Shin HS, Porter JE, Geiger JD & Lei S. (2010). Cholecystokinin facilitates glutamate release by increasing the number of readily releasable vesicles and releasing probability. J Neurosci 30, 5136–5148. [PubMed: 20392936]

Dorsa DM, Petracca FM, Baskin DG & Cornett LE. (1984). Localization and characterization of vasopressin-binding sites in the amygdala of the rat brain. J Neurosci 4, 1764–1770. [PubMed: 6330316]

Dumont EC, Martina M, Samson RD, Drolet G & Pare D. (2002). Physiological properties of central amygdala neurons: species differences. Eur J Neurosci 15, 545–552. [PubMed: 11876782]

Egashira N, Mishima K, Iwasaki K, Oishi R & Fujiwara M. (2009). New topics in vasopressin receptors and approach to novel drugs: role of the vasopressin receptor in psychological and cognitive functions. J Pharmacol Sci 109, 44–49. [PubMed: 19151541]

Egashira N, Tanoue A, Matsuda T, Koushi E, Harada S, Takano Y, Tsujimoto G, Mishima K, Iwasaki K & Fujiwara M. (2007). Impaired social interaction and reduced anxiety-related behavior in vasopressin V1a receptor knockout mice. Behav Brain Res 178, 123–127. [PubMed: 17227684]

Ehrlich I, Humeau Y, Grenier F, Ciocchi S, Herry C & Luthi A. (2009). Amygdala inhibitory circuits and the control of fear memory. Neuron 62, 757–771. [PubMed: 19555645]

Gilpin NW, Herman MA & Roberto M. (2015). The central amygdala as an integrative hub for anxiety and alcohol use disorders. Biol Psychiatry 77, 859–869. [PubMed: 25433901]

Grundy D (2015). Principles and standards for reporting animal experiments in The Journal of Physiology and Experimental Physiology. J Physiol 593, 2547–2549. [PubMed: 26095019]

Hammock EA, Lim MM, Nair HP & Young LJ. (2005). Association of vasopressin 1a receptor levels with a regulatory microsatellite and behavior. Genes Brain Behav 4, 289–301. [PubMed: 16011575]

Helliwell RM & Large WA. (1996). Dual effect of external Ca2+ on noradrenaline-activated cation current in rabbit portal vein smooth muscle cells. J Physiol 492 (Pt 1), 75–88. [PubMed: 8730584]

Hernandez-Perez OR, Crespo-Ramirez M, Cuza-Ferrer Y, Anias-Calderon J, Zhang L, Roldan-Roldan G, Aguilar-Roblero R, Borroto-Escuela DO, Fuxe K & Perez Mora M de la. (2018). Differential activation of arginine-vasopressin receptor subtypes in the amygdaloid modulation of anxiety in the rat by arginine-vasopressin. Psychopharmacology (Berl) 235, 1015–1027. [PubMed: 29306965]

Hibino H, Inanobe A, Furutani K, Murakami S, Findlay I & Kurachi Y. (2010). Inwardly rectifying potassium channels: their structure, function, and physiological roles. Physiol Rev 90, 291–366. [PubMed: 20086079]

Hofmann T, Obukhov AG, Schaefer M, Harteneck C, Gudermann T & Schultz G. (1999). Direct activation of human TRPC6 and TRPC3 channels by diacylglycerol. Nature 397, 259–263. [PubMed: 9930701]

Hopkins DA & Holstege G. (1978). Amygdaloid projections to the mesencephalon, pons and medulla oblongata in the cat. Exp Brain Res 32, 529–547. [PubMed: 689127]

Hu B, Boyle CA & Lei S. (2020). Oxytocin receptors excite lateral nucleus of central amygdala by phospholipase Cbeta- and protein kinase C-dependent depression of inwardly rectifying K(+) channels. J Physiol 598, 3501–3520. [PubMed: 32458437]

Huang CL, Feng S & Hilgemann DW. (1998). Direct activation of inward rectifier potassium channels by PIP2 and its stabilization by Gbetagamma. Nature 391, 803–806. [PubMed: 9486652]

Huber D, Veinante P & Stoop R. (2005). Vasopressin and oxytocin excite distinct neuronal populations in the central amygdala. Science 308, 245–248. [PubMed: 15821089]

Janak PH & Tye KM. (2015). From circuits to behaviour in the amygdala. Nature 517, 284–292. [PubMed: 25592533]

Johansen JP, Cain CK, Ostroff LE & LeDoux JE. (2011). Molecular mechanisms of fear learning and memory. Cell 147, 509–524. [PubMed: 22036561]

Just S, Chenard BL, Ceci A, Strassmaier T, Chong JA, Blair NT, Gallaschun RJ, Del Camino D, Cantin S, D'Amours M, Eickmeier C, Fanger CM, Hecker C, Hessler DP, Hengerer B, Kroker KS, Malekiani S, Mihalek R, McLaughlin J, Rast G, Witek J, Sauer A, Pryce CR & Moran MM. (2018). Treatment with HC-070, a potent inhibitor of TRPC4 and TRPC5, leads to anxiolytic and antidepressant effects in mice. PLoS One 13, e0191225. [PubMed: 29385160]

Kompier NF, Keysers C, Gazzola V, Lucassen PJ & Krugers HJ. (2019). Early Life Adversity and Adult Social Behavior: Focus on Arginine Vasopressin and Oxytocin as Potential Mediators. Front Behav Neurosci 13, 143. [PubMed: 31404254]

Koshimizu TA & Tsujimoto G. (2009). New topics in vasopressin receptors and approach to novel drugs: vasopressin and pain perception. J Pharmacol Sci 109, 33–37. [PubMed: 19151539]

Krettek JE & Price JL. (1978). A description of the amygdaloid complex in the rat and cat with observations on intra-amygdaloid axonal connections. J Comp Neurol 178, 255–280. [PubMed: 627626]

Landgraf R, Gerstberger R, Montkowski A, Probst JC, Wotjak CT, Holsboer F & Engelmann M. (1995). V1 vasopressin receptor antisense oligodeoxynucleotide into septum reduces vasopressin binding, social discrimination abilities, and anxiety-related behavior in rats. J Neurosci 15, 4250–4258. [PubMed: 7790909]

Le Gal LaSalle G, Paxinos G & Ben-Ari Y. (1978). Neurochemical mapping of GABAergic systems in the amygdaloid complex and bed nucleus of the stria terminalis. Brain Res 155, 397–403. [PubMed: 688023]

LeDoux JE. (2000). Emotion circuits in the brain. Annu Rev Neurosci 23, 155–184. [PubMed: 10845062]

LeDoux JE, Cicchetti P, Xagoraris A & Romanski LM. (1990). The lateral amygdaloid nucleus: sensory interface of the amygdala in fear conditioning. J Neurosci 10, 1062–1069. [PubMed: 2329367]

Li D, Jin T, Gazgalis D, Cui M & Logothetis DE. (2019a). On the mechanism of GIRK2 channel gating by phosphatidylinositol bisphosphate, sodium, and the Gbetagamma dimer. J Biol Chem 294, 18934–18948. [PubMed: 31659119]

Li H, Hu B, Zhang HP, Boyle CA & Lei S. (2019b). Roles of K(+) and cation channels in ORL-1 receptor-mediated depression of neuronal excitability and epileptic activities in the medial entorhinal cortex. Neuropharmacology 151, 144–158. [PubMed: 30998945]

Liebsch G, Wotjak CT, Landgraf R & Engelmann M. (1996). Septal vasopressin modulates anxiety-related behaviour in rats. Neurosci Lett 217, 101–104. [PubMed: 8916082]

Mak P, Broussard C, Vacy K & Broadbear JH. (2012). Modulation of anxiety behavior in the elevated plus maze using peptidic oxytocin and vasopressin receptor ligands in the rat. J Psychopharmacol 26, 532–542. [PubMed: 21890582]

Martina M, Royer S & Pare D. (1999). Physiological properties of central medial and central lateral amygdala neurons. J Neurophysiol 82, 1843–1854. [PubMed: 10515973]

McDonald AJ. (1998). Cortical pathways to the mammalian amygdala. Prog Neurobiol 55, 257–332. [PubMed: 9643556]

McDonald AJ & Augustine JR. (1993). Localization of GABA-like immunoreactivity in the monkey amygdala. Neuroscience 52, 281–294. [PubMed: 8450947]

McOmish CE, Burrows EL, Howard M & Hannan AJ. (2008). PLC-beta1 knockout mice as a model of disrupted cortical development and plasticity: behavioral endophenotypes and dysregulation of RGS4 gene expression. Hippocampus 18, 824–834. [PubMed: 18493969]

Meyer T, Wellner-Kienitz MC, Biewald A, Bender K, Eickel A & Pott L. (2001). Depletion of phosphatidylinositol 4,5-bisphosphate by activation of phospholipase C-coupled receptors causes slow inhibition but not desensitization of G protein-gated inward rectifier K+ current in atrial myocytes. J Biol Chem 276, 5650–5658. [PubMed: 11104770]

Murgatroyd C, Wigger A, Frank E, Singewald N, Bunck M, Holsboer F, Landgraf R & Spengler D. (2004). Impaired repression at a vasopressin promoter polymorphism underlies overexpression of vasopressin in a rat model of trait anxiety. J Neurosci 24, 7762–7770. [PubMed: 15342744]

Neugebauer V (2015). Amygdala pain mechanisms. Handb Exp Pharmacol 227, 261–284. [PubMed: 25846623]

Neugebauer V, Galhardo V, Maione S & Mackey SC. (2009). Forebrain pain mechanisms. Brain Res Rev 60, 226–242. [PubMed: 19162070]

Neugebauer V, Li W, Bird GC & Han JS. (2004). The amygdala and persistent pain. Neuroscientist 10, 221–234. [PubMed: 15155061]

Neumann ID & Landgraf R. (2012). Balance of brain oxytocin and vasopressin: implications for anxiety, depression, and social behaviors. Trends Neurosci 35, 649–659. [PubMed: 22974560]

Okada T, Shimizu S, Wakamori M, Maeda A, Kurosaki T, Takada N, Imoto K & Mori Y. (1998). Molecular cloning and functional characterization of a novel receptor-activated TRP Ca2+ channel from mouse brain. J Biol Chem 273, 10279–10287. [PubMed: 9553080]

Otsuguro K, Tang J, Tang Y, Xiao R, Freichel M, Tsvilovskyy V, Ito S, Flockerzi V, Zhu MX & Zholos AV. (2008). Isoform-specific inhibition of TRPC4 channel by phosphatidylinositol 4,5-bisphosphate. J Biol Chem 283, 10026–10036. [PubMed: 18230622]

Owsianik G, Talavera K, Voets T & Nilius B. (2006). Permeation and selectivity of TRP channels. Annu Rev Physiol 68, 685–717. [PubMed: 16460288]

Pape HC & Pare D. (2010). Plastic synaptic networks of the amygdala for the acquisition, expression, and extinction of conditioned fear. Physiol Rev 90, 419–463. [PubMed: 20393190]

Pare D & Smith Y. (1993). Distribution of GABA immunoreactivity in the amygdaloid complex of the cat. Neuroscience 57, 1061–1076. [PubMed: 8309543]

Penzo MA, Robert V & Li B. (2014). Fear conditioning potentiates synaptic transmission onto long-range projection neurons in the lateral subdivision of central amygdala. J Neurosci 34, 2432–2437. [PubMed: 24523533]

Petracca FM, Baskin DG, Diaz J & Dorsa DM. (1986). Ontogenetic changes in vasopressin binding site distribution in rat brain: an autoradiographic study. Brain Res 393, 63–68. [PubMed: 3730894]

Petrovich GD. (2011). Learning and the motivation to eat: forebrain circuitry. Physiol Behav 104, 582–589. [PubMed: 21549730]

Petrovich GD. (2013). Forebrain networks and the control of feeding by environmental learned cues. Physiol Behav 121, 10–18. [PubMed: 23562305]

Pitkänen A (2000). Connectivity of the rat amygdaloid complex. Oxford University Press., New York.

Pitkanen A, Stefanacci L, Farb CR, Go GG, LeDoux JE & Amaral DG. (1995). Intrinsic connections of the rat amygdaloid complex: projections originating in the lateral nucleus. J Comp Neurol 356, 288–310. [PubMed: 7629320]

Plant TD & Schaefer M. (2005). Receptor-operated cation channels formed by TRPC4 and TRPC5. Naunyn Schmiedebergs Arch Pharmacol 371, 266–276. [PubMed: 15902430]

Pravetoni M & Wickman K. (2008). Behavioral characterization of mice lacking GIRK/Kir3 channel subunits. Genes Brain Behav 7, 523–531. [PubMed: 18194467]

Ramanathan G, Cilz NI, Kurada L, Hu B, Wang X & Lei S. (2012). Vasopressin facilitates GABAergic transmission in rat hippocampus via activation of V(1A) receptors. Neuropharmacology 63, 1218–1226. [PubMed: 22884625]

Ressler KJ. (2010). Amygdala activity, fear, and anxiety: modulation by stress. Biol Psychiatry 67, 1117–1119. [PubMed: 20525501]

Riccio A, Li Y, Moon J, Kim KS, Smith KS, Rudolph U, Gapon S, Yao GL, Tsvetkov E, Rodig SJ, Van't Veer A, Meloni EG, Carlezon WA Jr., Bolshakov VY & Clapham DE. (2009). Essential role for TRPC5 in amygdala function and fear-related behavior. Cell 137, 761–772. [PubMed: 19450521]

Riccio A, Li Y, Tsvetkov E, Gapon S, Yao GL, Smith KS, Engin E, Rudolph U, Bolshakov VY & Clapham DE. (2014). Decreased anxiety-like behavior and Galphaq/11-dependent responses in the amygdala of mice lacking TRPC4 channels. J Neurosci 34, 3653–3667. [PubMed: 24599464]

Rodriguez-Menchaca AA, Adney SK, Zhou L & Logothetis DE. (2012). Dual Regulation of Voltage-Sensitive Ion Channels by PIP(2). Front Pharmacol 3, 170. [PubMed: 23055973]

Rohacs T (2013). Regulation of transient receptor potential channels by the phospholipase C pathway. Adv Biol Regul 53, 341–355. [PubMed: 23916247]

Rood BD, Stott RT, You S, Smith CJ, Woodbury ME & De Vries GJ. (2013). Site of origin of and sex differences in the vasopressin innervation of the mouse (Mus musculus) brain. J Comp Neurol 521, 2321–2358. [PubMed: 23239101]

Savander V, Go CG, LeDoux JE & Pitkanen A. (1995). Intrinsic connections of the rat amygdaloid complex: projections originating in the basal nucleus. J Comp Neurol 361, 345–368. [PubMed: 8543667]

Schaefer M, Plant TD, Obukhov AG, Hofmann T, Gudermann T & Schultz G. (2000). Receptor-mediated regulation of the nonselective cation channels TRPC4 and TRPC5. J Biol Chem 275, 17517–17526. [PubMed: 10837492]

Sheng ZF, Zhang H, Zheng P, Chen S, Gu Z, Zhou JJ, Phaup JG, Chang HM, Yeh ETH, Pan HL & Li DP. (2021). Impaired Kv7 channel activity in the central amygdala contributes to elevated sympathetic outflow in hypertension. Cardiovasc Res.

Shi W, Cui N, Shi Y, Zhang X, Yang Y & Jiang C. (2007). Arginine vasopressin inhibits Kir6.1/SUR2B channel and constricts the mesenteric artery via V1a receptor and protein kinase C. Am J Physiol Regul Integr Comp Physiol 293, R191–199. [PubMed: 17428891]

Silberman Y, Shi L, Brunso-Bechtold JK & Weiner JL. (2008). Distinct mechanisms of ethanol potentiation of local and paracapsular GABAergic synapses in the rat basolateral amygdala. J Pharmacol Exp Ther 324, 251–260. [PubMed: 17921186]

Smith CM & Lawrence AJ. (2018). Salt Appetite, and the Influence of Opioids. Neurochem Res 43, 12–18. [PubMed: 28646260]

Strubing C, Krapivinsky G, Krapivinsky L & Clapham DE. (2001). TRPC1 and TRPC5 form a novel cation channel in mammalian brain. Neuron 29, 645–655. [PubMed: 11301024]

Suh BC & Hille B. (2008). PIP2 is a necessary cofactor for ion channel function: how and why? Annu Rev Biophys 37, 175–195. [PubMed: 18573078]

Szot P & Dorsa DM. (1993). Differential timing and sexual dimorphism in the expression of the vasopressin gene in the developing rat brain. Brain Res Dev Brain Res 73, 177–183. [PubMed: 8353930]

Trebak M, Lemonnier L, DeHaven WI, Wedel BJ, Bird GS & Putney JW Jr. (2009). Complex functions of phosphatidylinositol 4,5-bisphosphate in regulation of TRPC5 cation channels. Pflugers Arch 457, 757–769. [PubMed: 18665391]

Tully K, Li Y, Tsvetkov E & Bolshakov VY. (2007). Norepinephrine enables the induction of associative long-term potentiation at thalamo-amygdala synapses. Proc Natl Acad Sci U S A 104, 14146–14150. [PubMed: 17709755]

Tye KM, Prakash R, Kim SY, Fenno LE, Grosenick L, Zarabi H, Thompson KR, Gradinaru V, Ramakrishnan C & Deisseroth K. (2011). Amygdala circuitry mediating reversible and bidirectional control of anxiety. Nature 471, 358–362. [PubMed: 21389985]

Veinante P & Freund-Mercier MJ. (1997). Distribution of oxytocin- and vasopressin-binding sites in the rat extended amygdala: a histoautoradiographic study. J Comp Neurol 383, 305–325. [PubMed: 9205043]

Veinante P, Yalcin I & Barrot M. (2013). The amygdala between sensation and affect: a role in pain. J Mol Psychiatry 1, 9. [PubMed: 25408902]

Venkatachalam K, Zheng F & Gill DL. (2003). Regulation of canonical transient receptor potential (TRPC) channel function by diacylglycerol and protein kinase C. J Biol Chem 278, 29031–29040. [PubMed: 12721302]

Wakatsuki T, Nakaya Y & Inoue I. (1992). Vasopressin modulates K(+)-channel activities of cultured smooth muscle cells from porcine coronary artery. Am J Physiol 263, H491–496. [PubMed: 1387293]

Wu LJ, Sweet TB & Clapham DE. (2010). International Union of Basic and Clinical Pharmacology. LXXVI. Current progress in the mammalian TRP ion channel family. Pharmacol Rev 62, 381–404. [PubMed: 20716668]

Wydeven N, Marron Fernandez Velasco E de, Du Y, Benneyworth MA, Hearing MC, Fischer RA, Thomas MJ, Weaver CD & Wickman K. (2014). Mechanisms underlying the activation of G-protein-gated inwardly rectifying K+ (GIRK) channels by the novel anxiolytic drug, ML297. Proc Natl Acad Sci U S A 111, 10755–10760. [PubMed: 25002517]

Xiao Y, Chen X, Zhang PA, Xu Q, Zheng H & Xu GY. (2016). TRPV1-mediated presynaptic transmission in basolateral amygdala contributes to visceral hypersensitivity in adult rats with neonatal maternal deprivation. Sci Rep 6, 29026. [PubMed: 27364923]

Xiao Z, Jaiswal MK, Deng PY, Matsui T, Shin HS, Porter JE & Lei S. (2012). Requirement of phospholipase C and protein kinase C in cholecystokinin-mediated facilitation of NMDA channel function and anxiety-like behavior. Hippocampus 22, 1438–1450. [PubMed: 22072552]

Xiong Z, Lu W & MacDonald JF. (1997). Extracellular calcium sensed by a novel cation channel in hippocampal neurons. Proc Natl Acad Sci U S A 94, 7012–7017. [PubMed: 9192683]

Yang LP, Jiang FJ, Wu GS, Deng K, Wen M, Zhou X, Hong X, Zhu MX & Luo HR. (2015). Acute Treatment with a Novel TRPC4/C5 Channel Inhibitor Produces Antidepressant and Anxiolytic-Like Effects in Mice. PLoS One 10, e0136255. [PubMed: 26317356]

Zanchi D, Depoorter A, Egloff L, Haller S, Mahlmann L, Lang UE, Drewe J, Beglinger C, Schmidt A & Borgwardt S. (2017). The impact of gut hormones on the neural circuit of appetite and satiety: A systematic review. Neurosci Biobehav Rev 80, 457–475. [PubMed: 28669754]

Zhang F, Mi Y, Qi JL, Li JW, Si M, Guan BC, Du XN, An HL & Zhang HL. (2013). Modulation of K(v)7 potassium channels by a novel opener pyrazolo[1,5-a]pyrimidin-7(4H)-one compound QO-58. Br J Pharmacol 168, 1030–1042. [PubMed: 23013484]

Zhu Y, Lu Y, Qu C, Miller M, Tian J, Thakur DP, Zhu J, Deng Z, Hu X, Wu M, McManus OB, Li M, Hong X, Zhu MX & Luo HR. (2015). Identification and optimization of 2-aminobenzimidazole derivatives as novel inhibitors of TRPC4 and TRPC5 channels. Br J Pharmacol 172, 3495–3509. [PubMed: 25816897]

Zschenderlein C, Gebhardt C, Bohlen Und Halbach O von, Kulisch C & Albrecht D. (2011). Capsaicin-induced changes in LTP in the lateral amygdala are mediated by TRPV1. PLoS One 6, e16116. [PubMed: 21249195]

Key Points Summary

- Activation of V_{1a} vasopressin receptors facilitates neuronal excitability in the medial nucleus of central amygdala (CeM)
- V_{1a} receptor activation excites about 80% CeM neurons by opening a cationic conductance and about 20% CeM neurons by suppressing an inwardly rectifying K^+ (Kir) channels
- The cationic conductance activated by V_{1a} receptors is identified as TRPC5 channels
- PLCβ-mediated depletion of PIP_2 is involved in V_{1a} receptor-elicited excitation of CeM neurons
- Intracellular Ca^{2+} release and PKC are unnecessary for V_{1a} receptor-mediated excitation of CeM neurons

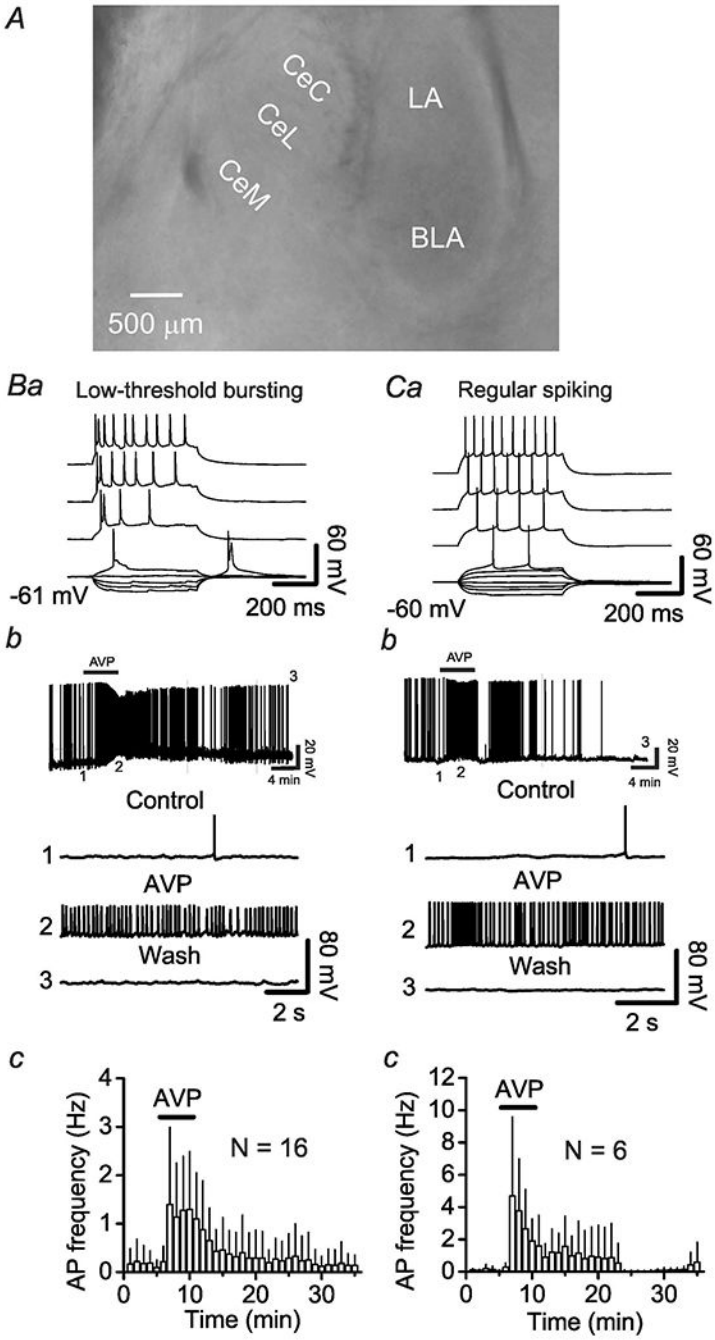

Figure 1. AVP increases AP firing frequency in CeM neurons.

A, microscopic photograph to show the location of CeM where electrophysiological recordings were conducted. LA: lateral nucleus; BLA: basolateral nucleus; CeC: capsular central amygdala; CeL: lateral central amygdala; CeM: medial central amygdala. ***Ba-c***, AVP enhanced AP firing frequency in low-threshold bursting (LTB) neurons. ***Ba***, Voltage responses were evoked by injection of currents at an increment of 30 pA from −90 pA to 120 pA. ***Bb***, Upper: APs recorded by injection of a persistent current of 50 pA before, during and after the application of AVP. Lower: expanded traces recorded at the time indicated in the

graph. ***Bc***, Averaged AP firing frequency recorded from 16 LTB neurons. ***Ca-c***, AVP enhanced AP firing frequency in regular spiking (RS) neurons. ***Ca***, Voltage responses were evoked by injection of currents at an increment of 30 pA from −90 pA to 180 pA. ***Cb***, Upper: APs recorded by injection of a persistent current of 90 pA before, during and after the application of AVP. Lower: expanded traces recorded at the time indicated in the graph. ***Cc***, Averaged AP firing frequency recorded from 6 RS neurons.

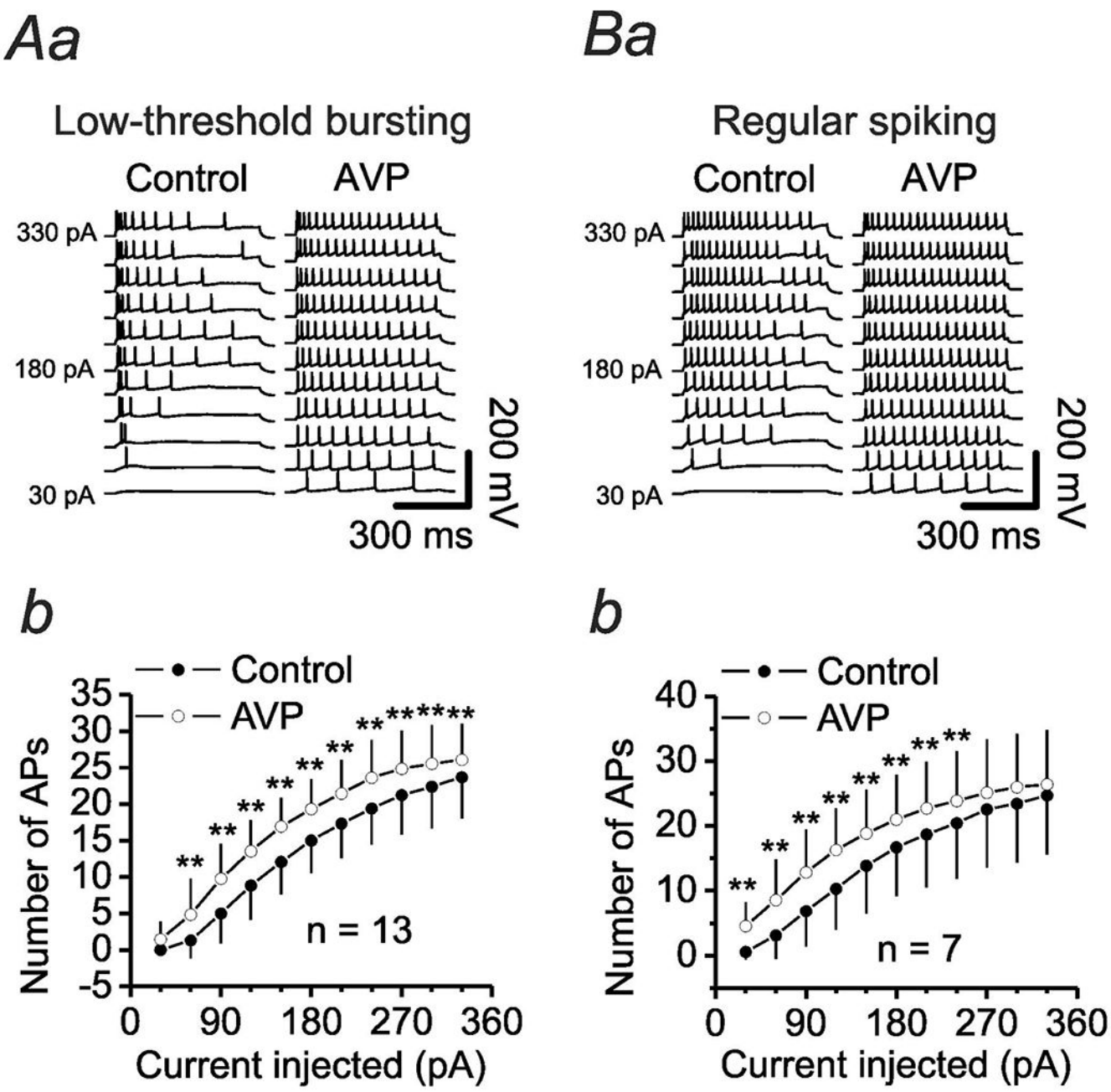

Figure 2. AVP increases the number of APs elicited by injection of a series of positive currents.

Aa-b, AVP enhanced the numbers of APs evoked by injections of positive currents from 30 pA to 330 pA in LTB neurons. ***Aa***, APs elicited by injections of a series of positive currents from 30 pA to 330 pA in a LTB neuron before (*left*) and during (*right*) the application of AVP. ***Ab***, Relationship between the injected currents and the elicited AP numbers from 13 LTB neurons. ** $P < 0.01$, Two-way repeated measures ANOVA followed by Sidak multiple comparison test. ***Ba-b***, AVP enhanced the numbers of APs evoked by injections of positive currents from 30 pA to 330 pA in RS neurons. ***Ba***, APs elicited by injections of a series of positive currents from 30 pA to 330 pA in a RS neuron before (*left*) and during (*right*) the

application of AVP. ***Bb***, Relationship between the injected currents and the elicited AP numbers from 7 RS neurons. ** $P < 0.01$, Two-way repeated measures ANOVA followed by Sidak multiple comparison test.

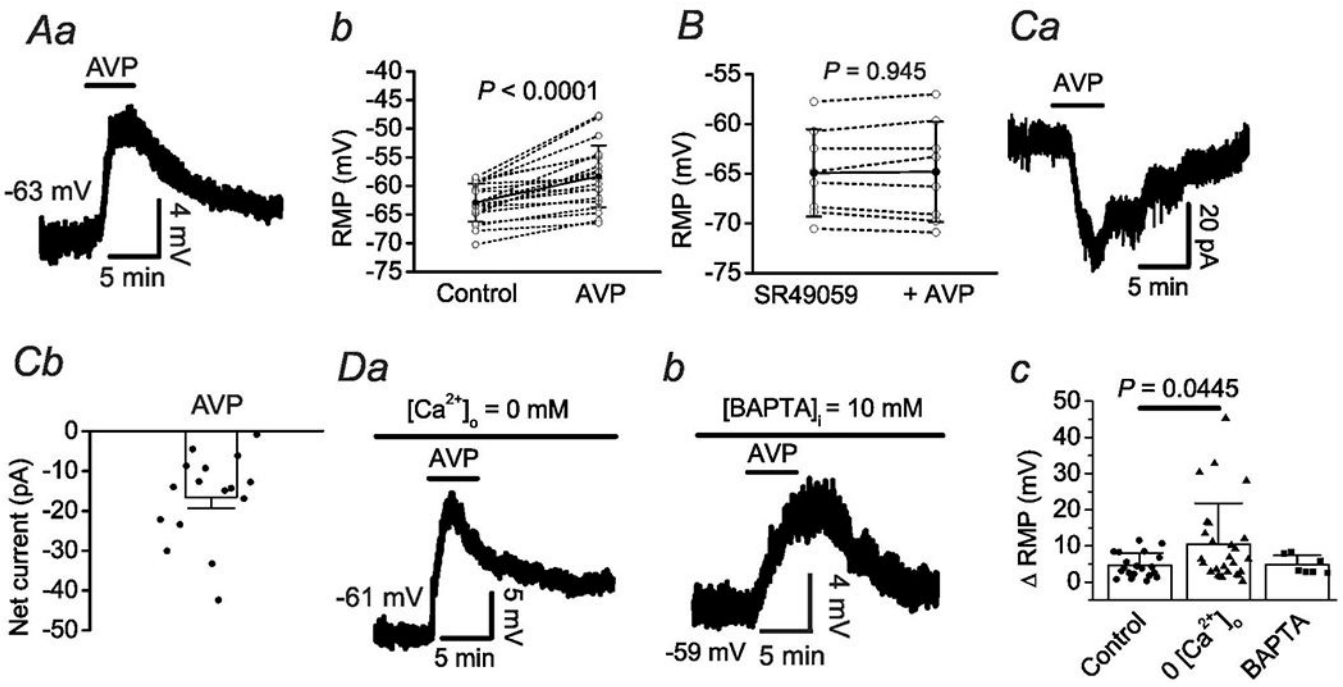

Figure 3. Involvement of V_{1a} receptors and effects of Ca^{2+} on AVP-mediated depolarization of CeM neurons.

Aa-b, Bath application of AVP depolarized CeM neurons. ***Aa***, RMP recorded from a CeM neuron before, during and after application of AVP. ***Ab***, Summary data for AVP-induced depolarization (Wilcoxon test). The empty circles represented the values from individual cells and the solid symbols were their averages. ***B***, Pretreatment of slices with and continuous bath application of the selective V_{1a} antagonist, SR49059 (1 μM), blocked AVP-induced depolarization (Wilcoxon test). ***Ca-b***, Bath application of AVP induced an inward current in voltage clamp. ***Ca***, Holding current recorded at −60 mV from a CeM neuron before, during and after the application of AVP. ***Cb***, Summary net currents induced by AVP recorded at −60 mV from 16 CeM neurons ($P < 0.0001$, Wilcoxon test). Circles represented the values from individual cells and bar graph was their average. ***Da-c***, AVP-elicited depolarization was augmented by removal of extracellular Ca^{2+}, but independent of intracellular Ca^{2+}. ***Da***, RMP recorded from a CeM neuron before, during and after application of AVP in the extracellular solution in which Ca^{2+} was substituted with the same concentration of Mg^{2+}. Note that AVP elicited a larger depolarization in the absence of extracellular Ca^{2+}. ***Db***, RMP recorded from a CeM neuron before, during and after application of AVP in the intracellular solution containing 10 mM BAPTA. ***Dc***, Summary data for AVP-induced depolarization in the extracellular solution containing no Ca^{2+} and intracellular solution containing 10 mM BAPTA (One-way ANOVA followed by Dunnett's test).

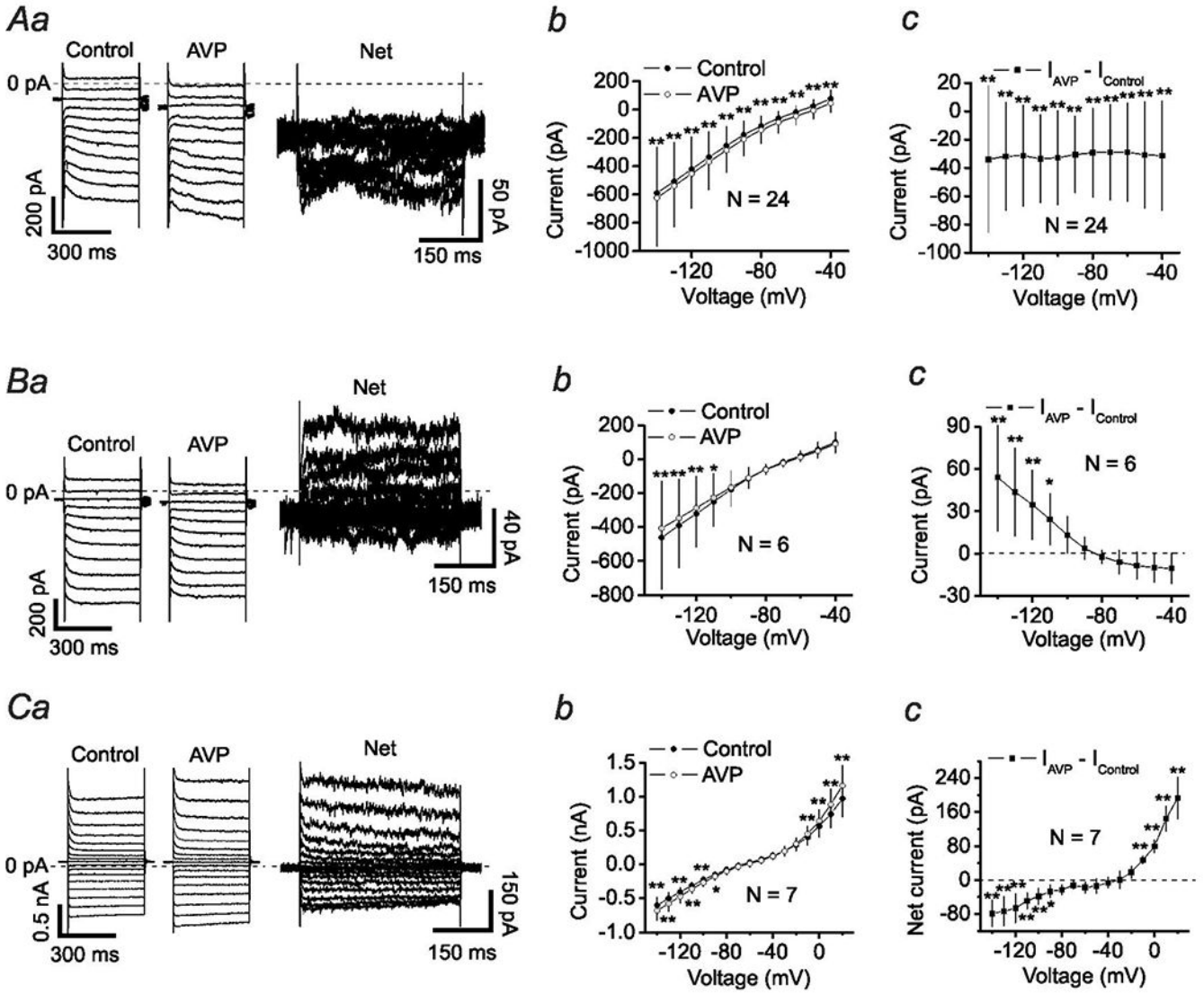

Figure 4. AVP-elicited excitation of CeM neurons is mediated by opening a cation channel and inhibiting a Kir channel.

Aa-c, AVP opened a cation channel. ***Aa***, Currents elicited by a voltage-step protocol before (*left*) and during (*middle*) bath application of AVP and the net current obtained by subtraction (*right*) from a CeM neuron. Note the differences of the scale bars. The dash line was the zero current level. ***Ab***, V-I curve averaged from 24 cells before and during application of AVP (Two-way repeated measures ANOVA followed by Sidak multiple comparison test; Drug: $F_{(1, 23)} = 28.83$, $P < 0.0001$; Voltage: $F_{(10, 230)} = 71.65$, $P < 0.0001$; Drug x Voltage: $F_{(10, 230)} = 0.134$, $P = 0.9993$; ** $P < 0.0001$). ***Ac***, V-I curve of the net current obtained by subtracting the currents in control condition from those after application of AVP. ***Ba-c***, AVP depressed a Kir channel. ***Ba***, Currents elicited by the voltage-step protocol before (*left*) and during (*middle*) bath application of AVP and the net current obtained by subtraction (*right*) from a CeM neuron. The dash line was the zero current level. ***Bb***, V-I curve averaged from 6 cells before and during application of AVP (Two-way repeated measures ANOVA followed by Sidak multiple comparison test; Drug: $F_{(1, 5)} =$

9.079, $P = 0.0296$; Voltage: $F_{(10, 50)} = 14.65$, $P < 0.0001$; Drug x Voltage: $F_{(10, 50)} = 11.19$, $P < 0.0001$; * $P = 0.011$, ** $P < 0.0001$). ***Bc***, V-I curve of the net current obtained by subtracting the currents in control condition from those during application of AVP. ***Ca-c***, AVP opened a double-rectified cation channel recorded in the extracellular solution containing 300 $BaCl_2$, 0.5 μM TTX, 200 μM $CdCl_2$ and 1 mM $NiCl_2$. ***Ca***, Currents elicited by the voltage-step protocol before (*left*) and during (*middle*) bath application of AVP and the net current obtained by subtraction (*right*) from a CeM neuron. The dash line was the zero current level. ***Cb***, V-I curve averaged from 7 cells before and during the application of AVP (Two-way repeated measures ANOVA followed by Sidak multiple comparison test; Drug: $F_{(1, 6)} = 1.332$, $P = 0.2924$; Voltage: $F_{(16, 96)} = 133.2$, $P < 0.0001$; Drug x Voltage: $F_{(16, 96)} = 78.31$, $P < 0.0001$; * $P = 0.032$, ** $P < 0.001$). ***Cc***, V-I curve of the net current obtained by subtracting the currents in control condition from those during application of AVP.

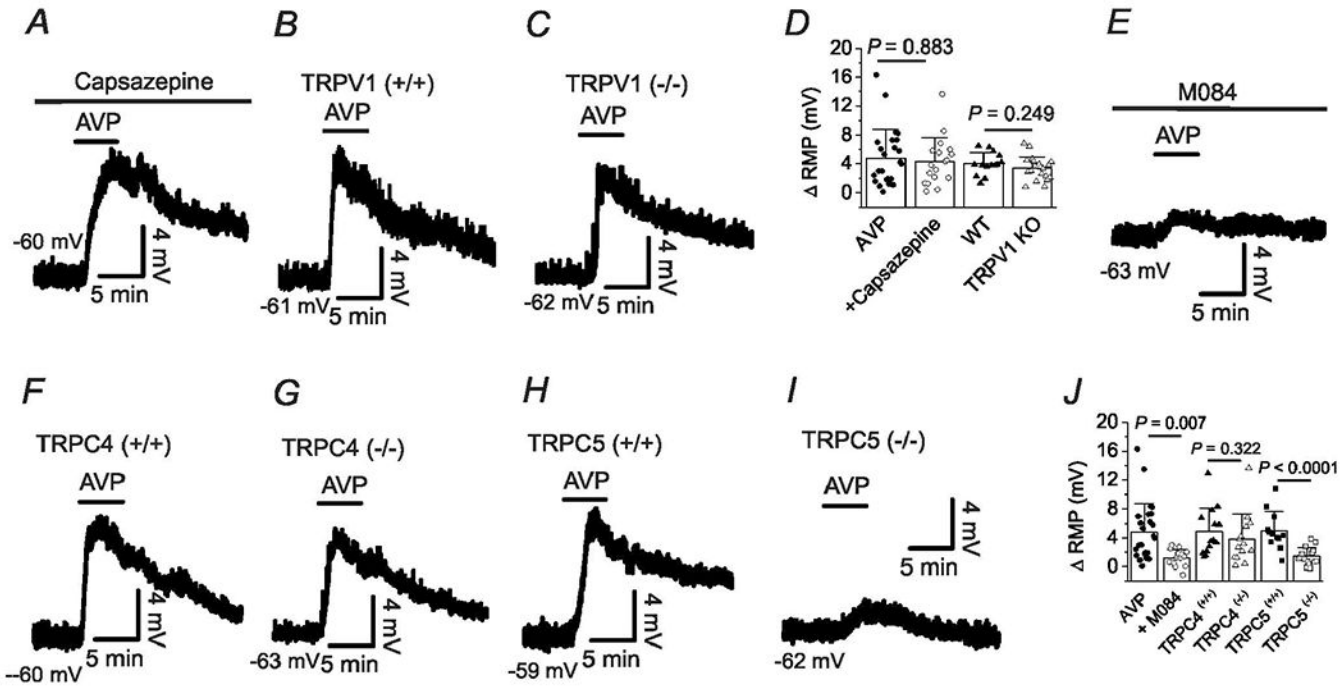

Figure 5. AVP-mediated depolarization is mediated by activation of TRPC5 channels.

A, RMP recorded from a CeM neuron in response to bath application of AVP in the continuous presence of capsazepine (10 μM). ***B***, RMP recorded from a CeM neuron in a slice cut from a WT mouse before, during and after application of AVP. ***C***, RMP recorded from a CeM neuron in a slice cut from a TRPV1 KO mouse before, during and after application of AVP. ***D***, Summary graph (Mann-Whitney test). ***E***, RMP recorded from a CeM neuron in response to bath application of AVP in the continuous presence of M084 (100 μM). ***F***, RMP recorded from a CeM neuron in a slice cut from a WT mouse prior to, during and after application of AVP. ***G***, RMP recorded from a CeM neuron in a slice cut from a TRPC4 KO mouse in response to AVP. ***H***, AVP-elicited response from a CeM neuron in a slice cut from a WT mouse. ***I***, RMP recorded from a CeM neuron in a slice cut from a TRPC5 KO mouse prior to, during and after application of AVP. ***J***, Summary graph (Mann-Whitney test).

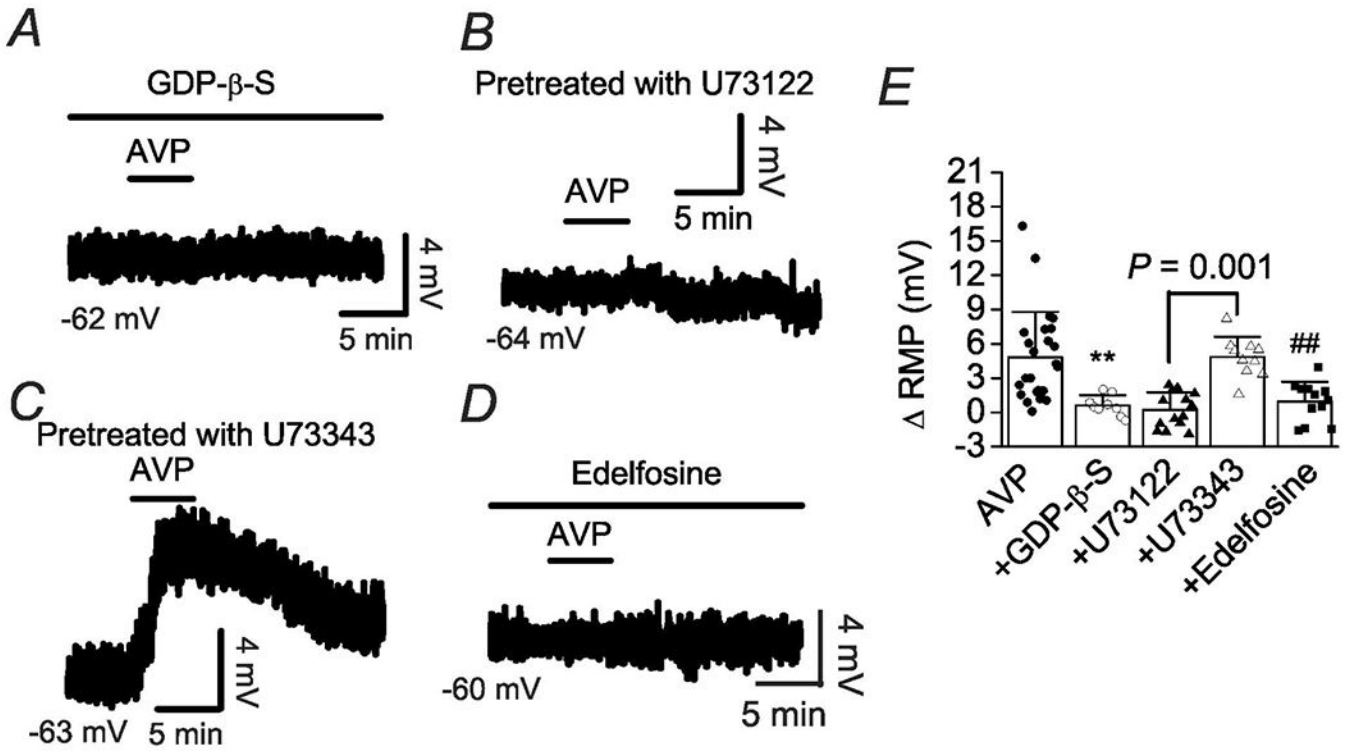

Figure 6. AVP-mediated depolarization of CeM neurons is dependent on G proteins and PLCβ.

A, Bath application of AVP did not induce depolarization recorded from a CeM neuron in a pipette containing GDP-β-S (0.5 mM). ***B***, Application of AVP did not elicit depolarization in a CeM neuron in a slice pretreated with U73122. ***C***, Application of AVP elicited depolarization in a CeM neuron in a slice pretreated with U73343. ***D***, AVP failed to depolarize a CeM neuron in a slice pretreated with edelfosine. ***E***, Summary data. ** $P = 0.002$, ## $P = 0.001$ vs. AVP alone (One-way ANOVA followed by Tukey's multiple comparison test).

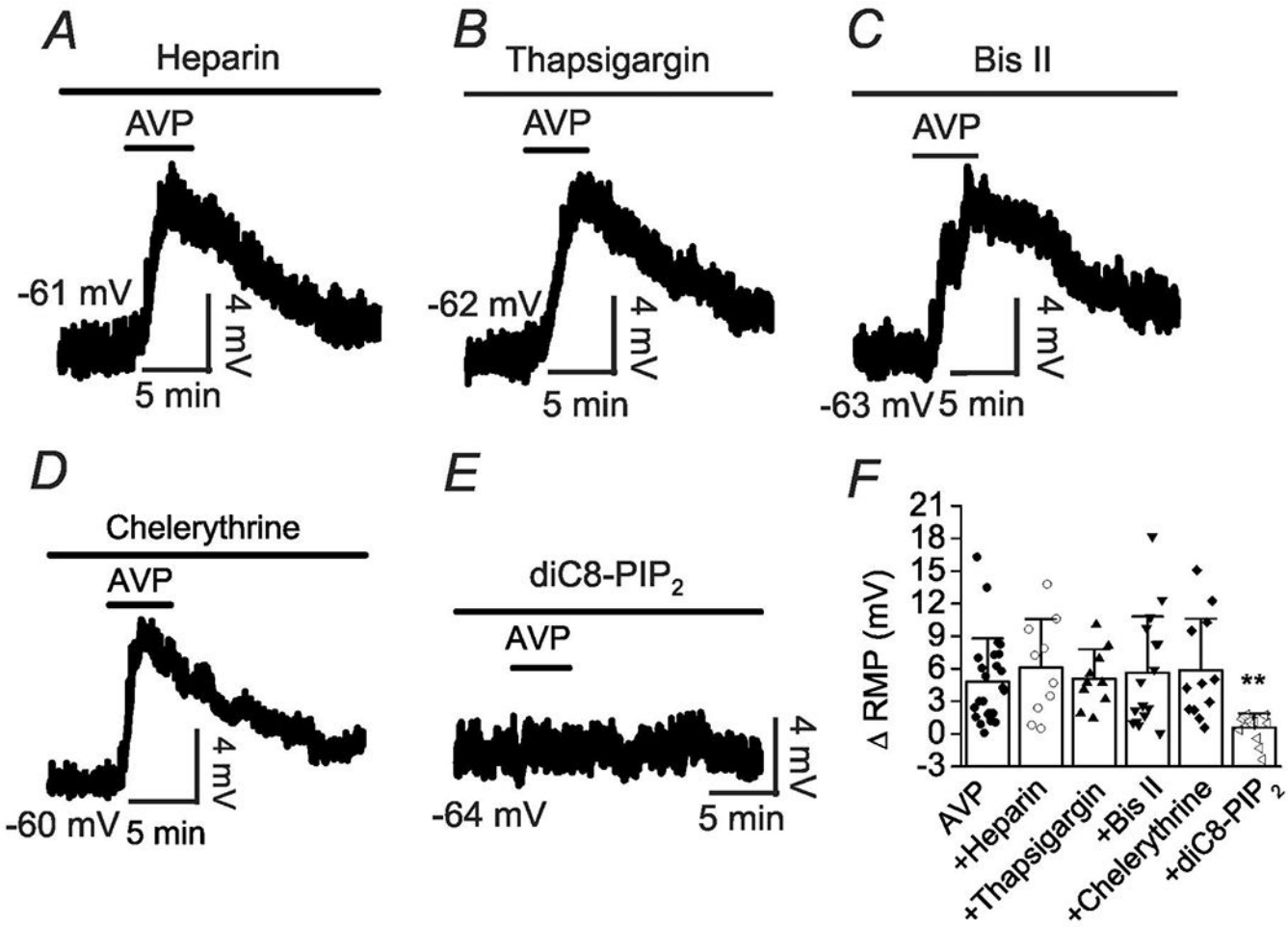

Figure 7. Intracellular Ca^{2+} release and PKC are not involved in AVP-mediated depolarization, whereas depletion of PIP_2 is required for AVP-elicited depolarization.

A, Intracellular dialysis of IP_3 receptor blocker, heparin (2 mg/ml), did not block AVP-induced depolarization. ***B***, Intracellular dialysis of the sarco-endoplasmic reticulum Ca^{2+}-ATPases inhibitor, thapsigargin (10 μM) failed to block AVP-elicited depolarization. ***C***, Pretreatment of slices with and continuous bath application of the selective PKC inhibitor, Bis II (1 μM), did not block AVP-mediated depolarization. ***D***, Pretreatment of slices with and continuous bath application of the selective PKC inhibitor, chelerythrine (10 μM), failed to block AVP-mediated depolarization. ***E***, Intracellular dialysis of diC8-PIP_2 (20 μM) blocked AVP-induced depolarization. ***F***, Summary data. ** $P = 0.008$ vs. AVP alone (One-way ANOVA followed by Dunnett's multiple comparison test).

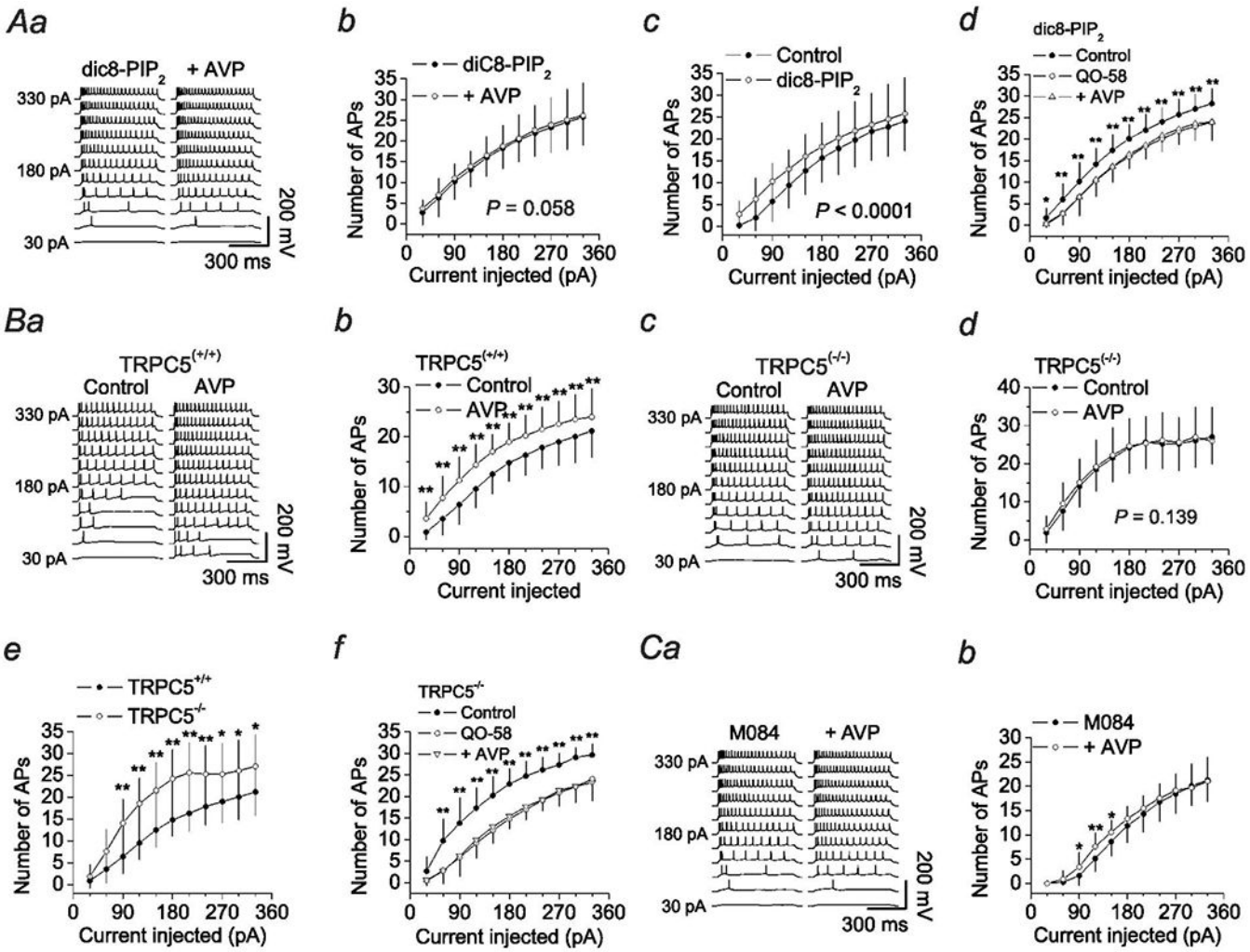

Figure 8. Roles of PIP_2, TRPC5 and Kir channels in AVP-induced augmentation of AP firing in CeM neurons.

Aa-d, Intracellular perfusion of diC8-PIP_2 blocked AVP-induced increases in AP firing of rat CeM neurons evoked by injections of positive currents from 30 pA to 330 pA at an increment of 30 pA every 10 s. ***Aa***, APs recorded by the protocol before (*left*) and during (*right*) the application of AVP from a rat CeM neuron dialyzed with diC8-PIP_2 (20 μM). ***Ab***, Relationship between the injected currents and the elicited AP numbers from 13 CeM neurons perfused with diC8-PIP_2 via the recording pipettes ($F_{(1,12)} = 4.38$, $P = 0.058$, Two-way repeated measures ANOVA followed by Sidak multiple comparison test). ***Ac***, Co-plot of the basal relationship of current injected and the number of APs elicited in control condition (data pooled from 13 LTB neurons and 7 RS neurons in Figure 2) and in the cells dialyzed with diC8-PIP_2 prior to AVP application ($F_{(1,341)} = 20.84$, $P < 0.0001$, Ordinary Two-way ANOVA followed by Sidak multiple comparison test. $P > 0.05$ for every pairwise comparison between control and diC8-PIP_2 at each current injected). ***Ad***, Bath application of QO-58 (15 μM), a Kv7 channel opener significantly decreased the number of APs in rat CeM cells dialyzed with diC8-PIP_2 (n = (12, 4), Two-way repeated measures ANOVA followed by Sidak multiple comparison test, $F_{(1,11)} = 137.7$, $P < 0.0001$; * $P = 0.021$, ** $P <$

0.0001 for the pairwise comparison at the currents injected between control and QO-58). Following application of AVP in the presence of both diC8-PIP_2 and QO-58 failed to increase AP numbers further ($F_{(1,11)} = 2.23$, $P = 0.164$, Two-way repeated measures ANOVA followed by Sidak multiple comparison test). ***Ba-f***, AVP increased the numbers of APs elicited by injections of the positive currents in CeM neurons of WT mice, but failed to enhance significantly those of TRPC5 KO mice. ***Ba***, APs recorded by the current injection protocol before (*left*) and during (*right*) the application of AVP from a WT CeM neuron. ***Bb***, Relationship between the injected currents and the elicited AP numbers from 15 cells of 5 WT mice (Two-way repeated measures ANOVA followed by Sidak multiple comparison test, $F_{(1,14)} = 45.5$, $P < 0.0001$, ** $P < 0.0001$ for the pairwise comparison at each current injected). ***Bc***, APs recorded by the current injection protocol before (*left*) and during (*right*) the application of AVP from a TRPC5 KO CeM neuron. ***Bd***, Relationship between the injected currents and the elicited AP numbers from 15 cells from 5 TRPC5 KO mice ($F_{(1,14)} = 2.46$, $P = 0.139$, Two-way repeated measures ANOVA followed by Sidak multiple comparison test). ***Be***, Co-plots of the relationship of current injected and the number of APs elicited in control condition prior to AVP application in the CeM neurons from WT mice (n = (15, 5)) and TRPC5 KO mice (n = (15, 5)) (Ordinary Two-way ANOVA followed by Sidak multiple comparison test, $F_{(1,308)} = 137.6$, $P < 0.0001$, * $P < 0.05$, ** $P < 0.01$ for the pairwise comparisons indicated at the currents injected). ***Bf***, Bath application of QO-58 (20 μM) significantly lowered the number of APs in TRPC5 KO CeM neurons (n = (12, 4), Two-way repeated measures ANOVA followed by Sidak multiple comparison test, $F_{(1,11)} = 153$, $P < 0.0001$, ** $P < 0.0001$ for the pairwise comparisons at the indicated currents injected between control and QO-58). Following application of AVP failed to enhance AP firing numbers significantly in TRPC5 KO CeM neurons (n = (12, 4), $F_{(1,11)} = 0.78$, $P = 0.397$, Two-way repeated measures ANOVA followed by Sidak multiple comparison test). ***Ca-b***, Depression of Kir channels contributed partially to AP-elicited facilitation of AP firing numbers in rat CeM neurons. ***Ca***, APs recorded from a rat CeM neuron evoked by the current injection protocol before (*left*) and during (*right*) the application of AVP in the continuous presence of M084 (100 μM) to block TRPC5 channels. Note that AVP increased AP numbers in response to injections of lower current intensities. ***Cb***, Relationship between the injected currents and the elicited AP numbers from 15 CeM cells of 4 rats prior to and during the application of AVP in the continuous presence of M084. Note that there was significant difference for the AP numbers when the injection currents were from 90 to 150 pA (Two-way repeated measures ANOVA followed by Sidak multiple comparison test, Drug: $F_{(1,14)} = 3.06$, $P = 0.102$; Current: $F_{(10,140)} = 188.2$, $P < 0.0001$; Drug x Current: $F_{(10,140)} = 2.432$, $P = 0.011$; * $P = 0.034$ at 90 pA, ** $P = 0.0007$ at 120 pA, * $P = 0.017$ at 150 pA).

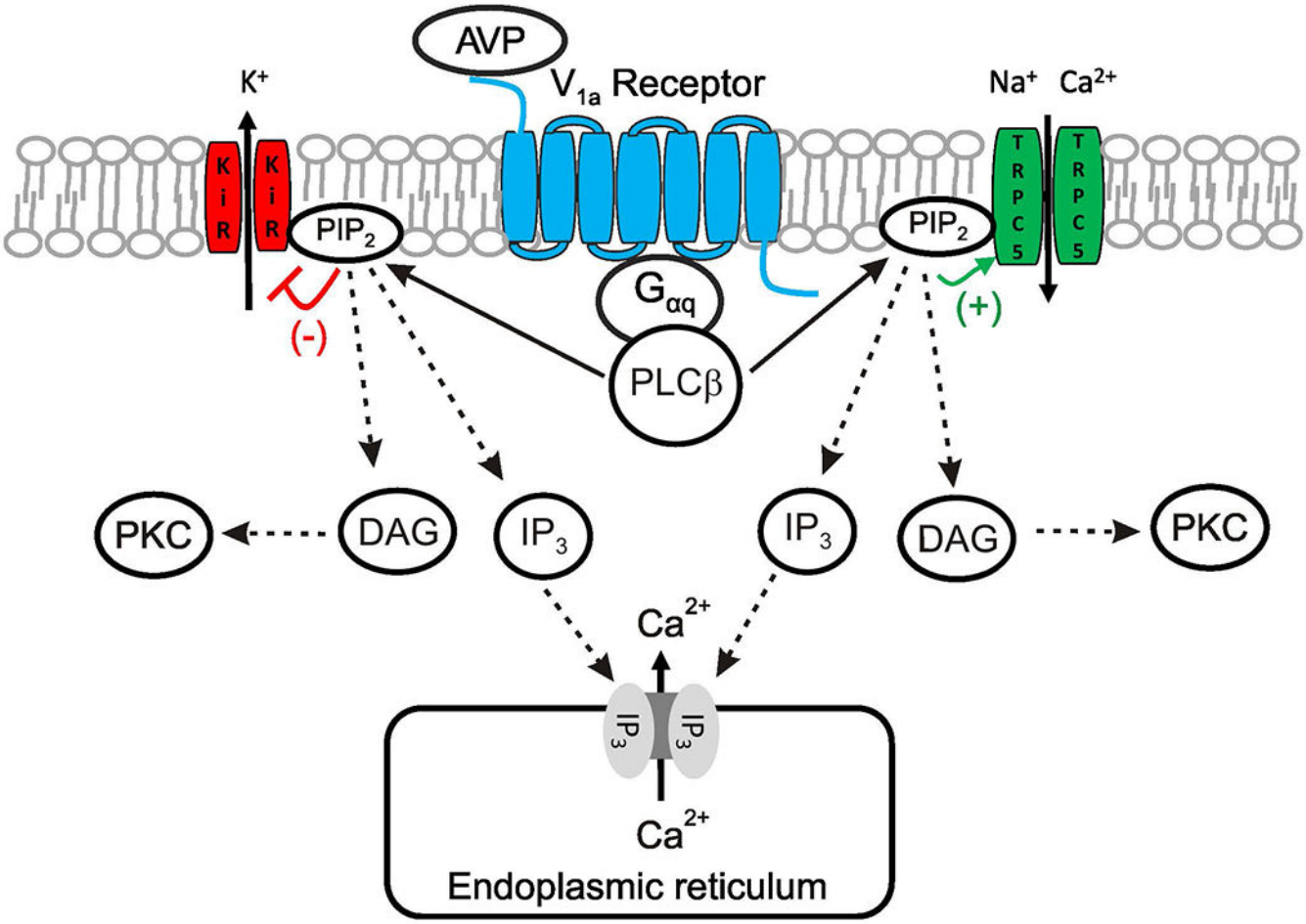

Figure 9. Schematic diagram illustrating the ionic and signaling mechanisms involved in AVP-mediated excitation of CeM neurons.

AVP activates V_{1a} receptors resulting in activation of $G\alpha_q$ proteins leading to increases in PLCβ activity. Activation of PLCβ catalyzes the hydrolysis of PIP_2 to generate IP_3 to increase intracellular Ca^{2+} release from IP_3-sensitive store and diacylglycerol (DAG) to activate protein kinase C (PKC). PLCβ-induced depletion of PIP_2 results in opening of TRPC5 channels and depression of Kir channels to excite CeM neurons. PKC and intracellular Ca^{2+} may have functions other than excite CeM neurons.